View metadata, citation and similar papers at core.ac.uk

brought to you by CORE

provided by NASA Technical Reports Server

CR-61628

BUBBLE FORMATION AND GROWTH

Study of the Boundary Conditions at a Liquid-Vapor Interface through Irreversible Thermodynamics

by

Ravinder K. Sakhuja

GPO PRICE $

CFSTI PRICE(S) $

Hard copy (HC) 3.00

Microfiche (MF) .65

ff 653 July 65

N68-18630

(ACCESSION NUMBER) 22 (PAGES) (NASA CR OR TMX OR AD NUMBER) CR-61628

(THRU) 1 (CODE) 33 (CATEGORY)

FACILITY FORM 602

Quarterly Progress Report

September - November 1967

for

National Aeronautics and Space Administration

George C. Marshall Space Flight Center

Huntsville, Alabama

Attn: Pr-EC

Contract No. NAS 8-20013

Control No. 1-5-52-01122-01 (1F)

January 1968

Department of Mechanical Engineering

Massachusetts Institute of Technology

MAR 1968

RECEIVED

NASA STI FACILITY

INPUT BRANCH

ABSTRACT

The purpose of this study is to investigate theoretically and experimentally the condensation coefficient and other transport coefficients appearing in linear irreversible thermodynamics rate equations of a phase change. The irreversible thermodynamics equations were derived by Bornhorst[8] as a result of an improved analysis for the process of phase change, compared to the kinetic analysis of Schrage[6]. Schrage had derived an equation for the rate of phase change which assumed maxwellian velocity distribution for the incoming vapor molecules striking the surface. The irreversible analysis did not assume any velocity distribution for vapor molecules but did satisfy the first and second laws of thermodynamics, which were not satisfied by the Schrage analysis.

Adt[9] measured the values of "σ" and "K," the transport coefficients appearing in the irreversible thermodynamics rate equation of a phase change, by performing a steady state evaporation of mercury. As a result of his experiments, the value of "σ" was found to be higher than that reported in the previous experiments (mainly condensation experiments) over the pressure range considered.

The steady state evaporation experiment has been performed for higher pressures ($\gtrsim$ 0.017 atm), and the average value of "σ" has been found to be 0.79, which is again higher than the values reported in previous experiments. There is, however, a very mild slope in the "σ"

versus pressure curve, which indicates the possibility of "σ" decreasing at higher pressures, though the decrease in value may not be as high as reported by other investigators.

A kinetic theory model has been developed to study the condensation process and the behaviour of condensation coefficient "σ" at higher values of pressure thereby showing that it is possible for the condensation coefficient to be less than unity.

The average value of other transport coefficient "K" has been found to be 0.36 compared to 0.28 reported in the previous steady state evaporation experiment for mercury.

TABLE OF CONTENTS

		Page
ABSTRACT		2
TABLE OF CONTENTS		4
LIST OF ILLUSTRATIONS		6
LIST OF SYMBOLS		7
I.	INTRODUCTION	10
I-1.	Nusselt's Analysis of Condensation	10
I-2.	Temperature Drop at Liquid-Vapor Interface	10
I-3.	Schrage's Kinetic Analysis of the Phase Change	11
I-4.	Linear Irreversible Thermodynamic Analysis of the Phase Change	13
I-5.	Steady State Evaporation Experiment	16
I-6.	Present Investigation	17
II.	STEADY STATE EVAPORATION EXPERIMENT	18
II-1.	Experimental Set-up	18
II-2.	Operating Procedure	20
II-3.	Steady State Equations and Expressions for Data Reduction	22
III.	EXPERIMENTAL RESULTS	26
IV.	DISCUSSION OF RESULTS	28
V.	KINETIC THEORY MODEL OF CONDENSATION	30
V-1.	Introduction	30
V-2.	Model and Its Assumptions	30
V-3.	Criterion for Sticking or Condensation	31
V-4.	Expression for Coefficient of Condensation	33
V-5.	Determination of V_{o*}	36
V-6.	Calculation of σ	38
V-7.	Checking of Assumption of $\mu < 1$	39

Page

VI. CONCLUSIONS 43

VII. RECOMMENDATIONS 44

BIBLIOGRAPHY 45

APPENDIX A - CONDENSATION OF EXPERIMENTAL ERRORS 47

A-1. Uncertainty Intervals 47
A-2. Important Errors in U 47
A-3. Important Errors in σ 48
A-4. Additional Errors 49

APPENDIX B - EVALUATION OF INTEGRAL APPEARING IN EQUATION (V-4-5) 51

TABLE 1 - Experimental Results 55

TABLE 2 Experimental Results 56

TABLE 3 Experimental Results 57

LIST OF ILLUSTRATIONS

Fig. No.		Page
1	Nusselt Model of Condensation	58
2	Schrage's Kinetic Model of Phase Change	59
3	Incorporation of Schrage's Kinetic Analysis in the Condensation Problem	60
4	Flow Diagram of Experiment	61
5	Photograph of Experimental Apparatus	62
6	Photograph of Test Section	63
7	Photograph of Test Section with Radiation Shield on the Thermocouple	64
8	Drawing of Test Section	65
9	Condensation Coefficient σ versus Pressure P_s for Various Liquid Metal	66
10	Condensation Coefficient σ versus Pressure P_s for Steady State Evaporation Experiment	67
11	Transport Coefficient U versus Pressure P_s for Steady State Evaporation Experiment	68
12	Model Showing the Collision between the Liquid Particle and Vapor Molecule	69
13	Mutual Force between the Liquid Particle and Vapor Molecule versus Relative Distance between Them	70
14	Condensation Coefficient σ versus Pressure P_s as Predicted by Kinetic Theory Metal	71
15	Model for Checking Assumption $\mu < 1$ Showing a Collision of Vapor Molecule with a Molecule in Liquid Lattice	72

LIST OF SYMBOLS

Symbol	
a	lattice spacing
C	speed of sound
E	energy of potential well
F	force
$f(u_o)$	velocity distribution function for a given u_o
$G(v_o)$	velocity distribution function for a given v_o
h	specific enthalpy
h_{fg}	$h_{fg} = h_g - h_f$
h_{Hg}	liquid depth
J_i	mass flux
J_s	$J_s \equiv P/\sqrt{2\pi RT}$
J_u	energy flux
K	transport coefficient
k	thermal conductivity
L_{ii}	transport coefficient
L_k	transport coefficient
ℓ	characteristic length of collision
M	mass of molecule
m	mass of liquid particle (Section V-2)
n	number of molecules
N_1	see Equation (V-4-3)
P	pressure

$P_c(u_o)$	probability of collision for a given u_o
$P_t(u_o)$	probability of trapping for a given u_o
R	gas constant
R_I	radius of influence
T	temperature
t	time
U	see Equation (II-3-4)
u_o	velocity of vapor molecule
u_1	velocity of vapor molecule after the collision
v_o	velocity of liquid particle
v_1	velocity of particle after the collision
V	velocity
δP	$\delta P \equiv P_g - P_s(T_{fi})$
δT	$\delta T \equiv T_{gi} - T_{fi}$
Γ	discussed under Equation (I-3-1)
γ	specific heat ratio c_p/c_v
κ	Boltzmann constant
η	see Equation (V-4-10)
μ	$\mu \equiv M/m$
ρ	density
σ	condensation of evaporation coefficient
τ	time interval of collision
ω	estimated error in experimental quantities

Subscripts

f	liquid
g	vapor
H	mercury
i	liquid vapor interface
max	maximum
min	minimum
NI	nickel
Na	sodium
ss	steady state
s	saturation condition
w	wall

I. INTRODUCTION

I-1. Nusselt's Analysis of Condensation

Nusselt[1] was first to analyse the problem of vapor condensing on a vertical flat plate. The model used in his analysis is illustrated in Fig. (1). He assumed continuous temperature profile from T_w, the wall temperature, to T_∞, the temperature of condensing vapor. Moreover, the condensing vapor was assumed to have uniform temperature distribution. This simple analysis was later modified to include various effects which Nusselt neglected. Among these were momentum effects (Sparrow and Gregg[2]), shear stress at liquid vapor interface (Chen[3], Koh[4], et al.) and non-linearity of the temperature distribution in the boundary layer[2]. Experiments with non-metallic liquids have shown good agreement with the theoretical predictions by the improved theories. For liquid metals, however, heat transfer coefficients have been reported to be five to thirty times lower than values predicted by the theory. This discrepancy has been attributed to some additional resistance to heat transfer.

I-2. Temperature Drop at Liquid-Vapor Interface

This additional resistance to heat transfer has been attributed in the literature (Kroger[5]) to the liquid-vapor interface. It manifests itself in terms of a temperature drop δT between the bulk flow region of liquid condensate film and bulk flow region of vapor. A nonequilibrium region is suspected to exist at the interface

because of net finite mass flux from one region to another by virtue of phase change. In such a nonequilibrium region, the temperature, chemical potential, and other thermodynamic properties are not defined. Also, the Fourier Law of heat conduction and other continuum equations do not hold. Because of finite mass flux and energy flux, a finite change in temperature and chemical potential across the nonequilibrium region is expected. Since the part of the temperature and chemical potential profile corresponding to this region is missing and since the nonequilibrium region is very thin (of the order of few mean free paths), it may be said, as a good approximation, that temperature and chemical potential vary discontinuously across the interface.

I-3. Schrage's Kinetic Analysis of the Phase Change

Schrage[6] derived an equation for the rate of phase change. His model is illustrated in Fig. (2). Near the interface, velocity distribution of the vapor molecules incident on liquid surface is assumed to be half maxwellian, characterised by vapor temperature Tg and pressure pg, with superposed bulk velocity. The outgoing mass flux crossing from left to right is assumed to consist of two parts. One of them comprises of the molecules emitted by the liquid surface at its temperature T_{fi} and the corresponding saturation pressure $P_s(T_{fi})$. The other part consists of those molecules which are reflected from the interface. The relation between the reflected and the incident flux is defined by way of the condensation coefficient σ as the ratio

of condensed flux to the incident flux. On integrating the assumed velocity distributions and incorporating the definition of σ, Schrage derives the following equation for the rate of phase change

$$J_i = \frac{\sigma}{\sqrt{2\pi R}} \left[\frac{P_g \Gamma}{T_g^{1/2}} - \frac{P_s}{T_{fi}^{1/2}}\right] \quad , \tag{I-3-1}$$

where Γ is a quantity that accounts for the bulk flow velocity assumed in the incident velocity distribution and where σ is assumed to depend on temperature T_{fi} alone (Reference (9)).

This equation can be linearised for small rates of phase change as follows. For small rates we have

$$\frac{\delta P}{P} \equiv \frac{P_{gi} - P_s}{P_{gi}} \simeq \frac{P_{gi} - P_s}{P_s} \ll 1 \quad , \tag{I-3-2}$$

$$\frac{\delta T}{T} \equiv \frac{T_{gi} - T_{fi}}{T_{gi}} \simeq \frac{T_{gi} - T_{fi}}{T_{fi}} \ll 1 \quad , \tag{I-3-3}$$

and

$$\Gamma \simeq 1 - \frac{J_i}{P_s} \sqrt{\frac{\pi R T_{fi}}{2}} \quad . \tag{I-3-4}$$

Using these approximations, Equation (I-3-1) becomes

$$J_i = \frac{2\sigma}{2 - \sigma} \frac{P}{\sqrt{2\pi R T}} \left(\frac{\delta T}{2T} - \frac{\delta P}{P}\right) \quad . \tag{I-3-5}$$

Sukhatme and Rohsenow[7] and Kroger[5] incorporated Equation (I-3-5) into Nusselt's analysis to account for the additional resistance at the interface. Fig. (3) shows that because of the existence of δT at the interface, there is a lower heat flux at the wall for the same temperature difference between the wall temperature and the gas temperature outside the boundary layer. In other words, existence of δT at the interface reduces the driving force for the heat transfer. Assuming that the temperature in vapor is uniform, as in Nusselt's analysis, and that the energy flux J_u is given by $h_g J_i$, we can calculate σ from Schrage's equation (I-3-1) and experimental values for T_{gi}, the heat flux, T_w and T_{fi} (calculated from Nusselt's theory) and, therefore, $P_s(T_{fi})$.

I-4. Linear Irreversible Thermodynamic Analysis of the Phase Change

Bornhorst[8] presented an analysis of the phase change based on the principles of irreversible thermodynamics. The solution contains an equation for the rate of phase change very similar to the linearised Schrage equation (I-3-5). In the analysis, however, no velocity distribution for the molecules has to be assumed. In addition, the analysis yields an equation for energy flux J_u. The equations are as follows:

$$J_i = RL_{ii}\left[\frac{2h_{fg}}{RT}\left(\frac{K}{K+1}\right)\frac{\delta T}{2T} - \frac{\delta P}{P}\right] \qquad \text{(I-4-1)}$$

$$J_u = [h_{gi} - \frac{K}{K+1} h_{fg}] J_i - \frac{L_k}{T} \frac{\delta T}{T} \qquad (I-4-2)$$

h_{gi} and h_{fi} being the enthalpy of the vapor and liquid, respectively, at the interface and $h_{fg} = h_{gi} - h_{fi}$.

L_{ii}, K, L_k which appear in the above Equations (I-4-1) and (I-4-2) are thermodynamic properties called transport coefficients and have to be determined experimentally. The analysis is restricted to processes which are not inherently non-linear (see Reference (8), (9)). For physical meaning of these transport coefficients, see Reference (9). They have been defined as follows:

From Equation (I-4-1) we get

$$L_{ii} = - \frac{(J_i)_{\delta T=0} \, P}{R(\delta P)_{\delta T=0}} \quad . \qquad (I-4-3)$$

Comparing Equations (I-4-1) and (I-3-5), we get

$$L_{ii} = \frac{2\sigma}{2 - \sigma} \frac{P}{R\sqrt{2\pi RT}} \quad . \qquad (I-4-4)$$

From Equation (I-4-2), we get

$$L_k = - \frac{(J_u)_{J_i=0}}{(\delta T)_{J_i=0}} \, T^2 \qquad (I-4-5)$$

From the Equation (I-4-5) we see that L_k is a measure of the conductance of interface to heat transfer.

Kennard[10] related L_k to energy accommodation coefficient α by way of the temperature jump analysis. The result is as follows:

$$L_k = \left(\frac{\gamma + 1}{\gamma - 1}\right) \sqrt{\frac{R}{2\pi}}\ T^{3/2}\ P\left(\frac{\alpha}{2 - \alpha}\right) \qquad \text{(I-4-6)}$$

where

$\gamma = c_p/c_v$ for gas phase. The energy accommodation coefficient should be close to unity for a liquid vapor interface, particularly for a high molecularweight fluid[9].

$$(J_u)_{\delta T=0} = h_{gi}(J_i)_{\delta T=0} - \left(\frac{K}{K + 1}\right) h_{fg}(J_i)_{\delta T=0} \cdot \qquad \text{(I-4-7)}$$

The Equation (I-4-7) shows K as a measure of how the heat of vaporization splits at the interface for the zero δT. In other words, $K/(K+1)$ is is the fraction of the energy $h_{fg}\ J_i$ necessary for evaporation which is transferred to the interface from the vapor side, while the remaining is supplied by the liquid side.

Because of existence of K, we do not, in general, have uniform temperature profile in vapor. There will be a gradient in the vapor temperature at the interface to account for the heat transfer from the gas side, and the gradient can be positive or negative depending upon heat transfer on the gas side. Eventually it is expected to fall off exponentially with distance[9] from interface; therefore it is very hard to measure T_{gi}.

Thermodynamic analysis is more general than Schrage's theory because it does not have to assume any velocity distribution. The kinetic analysis is based on the definition of "σ" whereas the

transport coefficients appearing in the thermodynamic analysis are thermodynamic properties within the framework of linear assumptions. The thermodynamic analysis satisfies I and II laws by following the formulation of irreversible thermodyanmics which essentially results in the Onsager reciprocal law. Schrage does not satisfy these laws.

I-5. Steady State Evaporation Experiment

Adt[9] measured the coefficients σ and K experimentally by steady state evaporation of mercury in the pressure (saturation pressure corresponding to T_{fi}) range of 0.01 - 0.017 Atm. He was the first to determine the value of transport coefficient K, appearing in the irreversible thermodynamics analysis of the phase change. The description of his experiments has been outlined in the next section.

In the evaporation experiment, many errors which could appear in the condensation experiments can be eliminated. The major problem, which is suspected to exist in all condensation experiments, is due to the presence of non-condensable gases. They present an additional resistance to the flow of vapor because vapor has to diffuse through non-condensable gases to condense on the cold surface. These non-condensable gases accumulate near the condensing surface and form a blanket of high resistance which obstructs the flow of vapor, and partial pressure of the vapor decreases significantly near the interface. This results in the reduced value of heat transfer coefficient and also reduced value of σ.

In Adt's[9] evaporation experiment, mercury vapors move away from the interface, and the non-condensables do not accumulate near the interface. Also, it is a flow process, and there is no surface contamination due to stagnant film. The mercury inflow is more than the amount that evaporates, and all the time mercury evaporates from the fresh surface. Because the surface is being flushed with fresh mercury, the chances of surface contamination are greatly reduced. So overall, the evaporation experiment is less likely to contaminate than the condensation experiment.

I-6. Present Investigation

The purpose of the present investigation is to find the values of the condensation coefficient "σ" and the transport coefficient K in the higher pressure range (> 0.017 Atm), using the experimental techniques of Adt[9]. The data obtained by other experiments (mainly condensation experiments) so far show a decreasing value of σ at higher saturation pressures. Consequently, the values of σ at higher values of pressure are rather important in order to ascertain whether the value of condensation coefficient really decreases at higher pressures or not. The results are as discussed in Section IV. A kinetic model is then developed to show the possibility of condensation coefficient having a value less than unity.

II. STEADY STATE EVAPORATION EXPERIMENT

II-1. Experimental Set-up

The steady state phase change experiment is one in which the liquid changes to vapor phase at constant rate. It can be shown from the first law of thermodynamics[9] that if vapor temperature is assumed to be constant at a distance very far from the interface, it will be the same up to the vapor side of the interface. (Of course, in the nonequilibrium region, the temperature and other thermodynamic properties are not defined.) In the steady state evaporation, therefore, there is no temperature gradient in the vapor beyond a few mean free paths away from the interface.

The experiment performed is described in the succeeding paragraphs. For details, see reference (9).

The flow diagram of the experiment is shown in Fig. (4), and the sketch of the test section and photographs of the apparatus are illustrated in Figs. 5, 6, 7, and 8. Triply distilled liquid mercury is fed into the test section to flow over a nickel surface in the form of a thin layer. The nickel block is being heated by the electrical heaters placed near the bottom of the block. Temperature in the block is measured by the thermocouples placed in the block. The temperature profile in the block is extrapolated to the surface of the block. This temperature profile is further extrapolated through the liquid layer to find the temperature T_{fi} on the liquid side of the interface. The depth of the liquid layer was measured by the needle depth probe which

is spring mounted to the micrometer head as it is moved from the solid surface to the liquid surface by means of the micrometer head. In the extrapolation from solid to liquid temperature, it was assumed that solid liquid interface does not have any significant contact resistance. This assumption was verified experimentally.

The choice of nickel was made because mercury wets nickel. This is essential in order to have a thin film of liquid and to reduce the solid liquid contact resistance. A thin layer will reduce the errors due to the non-linear temperature profile and also the possibility of convection. In addition to this, the amount of superheat at solid surface being less, the chances of having nucleation sites for boiling will also decrease.

The depth of liquid layer is controlled by the inclination of the nickel block and by adjusting the flow rate. The flow rate of liquid into the test section is more than that evaporated, and the extra amount of mercury is collected in an overflow tank. The flow was adjusted through a micrometer valve very precisely.

The vapor temperature T_g is measured by means of copper constantan thermocouples enclosed in stainless steel sheaths located at different positions and orientations. The thermocouples were calibrated against a standard platinum resistance thermometer.

The pressure p_g in the test section is measured by a monometer whose one leg is connected to the test section and the other one to a plenum chamber kept at very low pressure (of the order of 25-30 microns) by a vacuum pump.

The vapor formed in the test section goes into a counter-flow water-cooled condenser. The condenser is further connected to an ice trap and a mercury filter; on to a vacuum pump exhausting into the laboratory exhaust system.

The test section is enclosed in a glass cylinder, covered by stainless steel plates at top and bottom. Heating tapes are wrapped around the cylinder and top and bottom plates to compensate for the heat loss to the surroundings and keep the test section temperature uniform. Two to three layers of fiberglas insulation are put around the test section to reduce the heat loss to the surroundings.

II-2. Operating Procedure

The procedure is briefly discussed as follows:

All parts are first cleaned with hydrochloric acid, acetone, and Trichloroethylene. The valve to the overflow collector tank (Fig. (4)) is closed, and mercury is allowed to flow over the nickel block. In order to have mercury wet the surface, the surface is rubbed with hydrochloric acid at the non-wetting spots. A thin layer of mercury has to be retained over the whole surface because once it stops wetting the surface, the system has to be taken apart to have mercury wet the surface again as it does not wet by itself.

The heating tapes are supplied with power to bring the gas temperature inside the apparatus to roughly a value at which the experiment is to be run. This temperature refers to liquid vapor interface temperature. It takes about two days to bring the apparatus to a steady state temperature of the order of 400 ^{o}F.

The operating procedure from there on is as follows:

a. Condenser cooling water is turned on, and ice is fed to the ice trap and to the thermocouple reference junction.

b. Vacuum pump "A" is used to bring the system pressure to the desired value determined by the saturation pressure, and once it is brought to that pressure level, it is kept open a little to purge any extra gases which might leak into the system.

c. The heaters in the nickel block are turned on. The input wattage determines the heat flux, and hence the rate of evaporation inside the test section. With the advent of evaporation, the pressure mounts up and so does the vapor temperature which is immediately sensed by the horizontal thermocouple. The vertical thermocouple was rather insensitive to the vapor temperature, being more close to the surrounding temperature. The pressure level in the test section was adjusted by valve "1" so that the two thermocouples read the same value during the test. Radiation shields were later put over the thermocouples, and it was discovered that radiation does not change the result. The horizontal thermocouple's sensitivity to the vapor temperature played a very important role in achieving the steady state condition. This shows that thermocouples were not locked by some temperature other than the vapor temperature. The experiment performed with the radiation shield to check the effects of radiative heat transfer lent complete support to this belief.

d. Once the pressure level is set, the depth of mercury was measured by means of a depth probe. Pressure and temperature measurements were made by means of a manometer and thermocouples.

It usually takes about one to two hours to achieve the steady state, and mercury is recleaned and reoxidized to be run into another test.

II-3. Steady State Equations and Expressions for Data Reduction

For steady state evaporation, there is no temperature gradient and hence no heat transfer in the vapor at the interface. The energy flux in the vapor bulk flow region is given by

$$(J_u)_{ss} = h_g \, (J_i)_{ss}$$

where subscript ss stands for steady state evaporation, and so from the energy Equation (I-4-3), we can see that heat transfer contribution in the vapor due to splitting of $h_{fg} \, J_i$ is balanced by the amount of heat transfer into the vapor due to conductance of the surface; that is,

$$\frac{K}{K+1} \; h_{fg} \; J_i = - \frac{L_k}{T^2} \, (\delta T)_{ss} \qquad \text{(II-3-1}$$

$$\frac{K}{K+1} = - \frac{1}{h_{fg}} \; \frac{L_k}{T^2} \, \left(\frac{\delta T}{J_i}\right)_{ss} \; . \qquad \text{(II-3-2)}$$

The rate of phase change, Equation (I-4-1), for steady state becomes

$$(J_i)_{ss} = L_{ii} R[\frac{2 h_{fg}}{RT} (\frac{K}{K+1}) \frac{(\delta T)_{ss}}{2T} - \frac{(\delta P)_{ss}}{P}] \quad . \qquad \text{(II-3-3)}$$

In place of K, another factor U, which is more convenient to handle, was defined.

$$U = \frac{K}{K+1} \frac{2 h_{fg}}{RT} \quad . \qquad \text{(II-3-4)}$$

For steady state experiment, combining Equations (II-3-2) and (II-3-4), we end up with

$$U = - \frac{2 L_k}{RT^3} \cdot (\frac{\delta T}{J_i})_{ss} \quad . \qquad \text{(II-3-5)}$$

For the value of L_k Equation (I-4-6) is used. Teagon's[11] work has found Kennard's[10] result to be quite satisfactory (within $\pm$ 4%) for solid vapor interface. It is expected that Kennard's analysis would be accurate for liquid vapor phase change, particularly for mercury with high molecular weight[9].

Substituting Equation (I-4-6) for L_k with $\alpha = 1$ into Equation (II-3-5), we have

$$U = - (\frac{\gamma + 1}{\gamma - 1}) \sqrt{\frac{2}{\pi R}} \frac{P}{T^{3/2}} (\frac{\delta T}{J_i})_{ss} \quad . \qquad \text{(II-3-6)}$$

Replacing L_{ii} with σ as it appears in Schrage's analysis, Equation (I-3-5), we have

$$\frac{2\sigma}{2-\sigma} = (J_i)_{ss} \frac{\sqrt{2\pi RT}}{P} \left[\frac{(\delta T)_{ss}}{2T} - \frac{(\delta P)_{ss}}{P}\right]^{-1} \qquad \text{(II-3-7)}$$

It was found experimentally that the value of $\frac{(\delta T)_{ss}}{2T}$ was an order of magnitude less than $\frac{(\delta P)_{ss}}{P}$, and coefficient U, which was assumed to be 1 by Schrage, does not change σ significantly.

The needed measurements to evaluate σ and U from Equations (II-3-7) and (II-3-6) are those of J_i, T_{fi}, T_{gi}, and P. P and T_{gi} are directly measured by manometer and thermocouples in the vapor. T_{fi} is measured by extrapolation of the temperature profile in the nickel block. By putting a least square straight line fit and then further extrapolating it through mercury, we have

$$T_{fi} = T_{Ni} - \left(\frac{k_{NI}}{k_{Hg}}\right) \left(\frac{\Delta T}{\Delta x}\right)_{Ni} h_{Hg} \qquad \text{(II-3-8)}$$

$$(\delta T)_{ss} = (T_{gi} - T_{fi}) \qquad \text{(II-3-9)}$$

and

$$(\delta P)_{ss} = P - P_s(T_{fi}) \qquad \text{(II-3-10)}$$

where $P_s(T_{fi})$ is the saturation pressure of mercury corresponding to temperature T_{fi}. The saturation pressure data was taken from reference (12). The rate of evaporation $(J_i)_{ss}$ is obtained from

$$(J_i)_{ss} = \frac{k_{NI}}{h_{fg}} \left(\frac{\Delta T}{\Delta x}\right)_{Ni} . \qquad \text{(II-3-11)}$$

The data for properties of nickel were taken from reference (13) and for other properties of mercury from reference (14).

III. EXPERIMENTAL RESULTS

The results have been given in Tables 1, 2, and 3 and have been plotted in Figs. 9, 10, and 11. The average value of condensation coefficient σ is 0.78, which is higher than that found in any previous condensation experiments performed in the pressure range considered. The σ reported in tests No. 1 and 2 has been found to be quite low. After these tests the mercury was taken out of the apparatus and was oxidized and redistilled, and also, all mercury lines in the apparatus were recleaned with hydrochloric acid and trichloroethylene. After that the value of σ was never found to be lower than 0.70. This again emphasizes the importance of contamination in the phenomenon of condensation and evaporation. The previous evaporation experiment performed by Adt[9] reported the added resistance due to stagnant film on the surface. This film is suspected to act as an obstacle in the way of evaporation and tends to reduce the value of condensation coefficient σ. In this experiment no stagnant film was observed, but the rise in the value of σ found after redistilling mercury can be attributed to the removal of some dissolved impurities which might have been present. It is believed that these impurities can have the effect of an added resistance and result in a lower value of σ.

The values of U have also been reported in Table 1. The average value of U was found to be 0.36 which is slightly higher than the one reported in the previous evaporation experiment by Adt[9].

The total percentage errors in U and σ have been reported in Table 2.

IV. DISCUSSION OF RESULTS

The value of condensation coefficient σ has been found to be higher than that found in the previous condensation experiments, and also, it has been shown at the same time that the contamination could cause the value of σ to decrease. The same result has been found by Adt[9] and Knudson[15]. Knudson, while performing the experiment with the evaporation of mercury, obtained the value of σ much less than 1 and later discovered that the surface of his drop was contaminated. Later he changed his drop every four seconds and found the results which gave σ very close to unity.

Kroger[4] introduced the non-condensable gases intentionally in the condensation of potassium and found out that σ decreased in their presence. Any non-condensables in the condensation experiments tend to collect on the surface, and the vapor has to diffuse through stagnant film of non-condensables.

This offers an extra resistance to the vapor passage, resulting in a lower value of σ. In the evaporation experiment the non-condensables do not present that much of a problem because the vapors move away from the surface, and hence flow being outward, the non-condensables do not accumulate at the surface.

As has also been found, the dissolved impurities can also reduce the value of σ. Consequently, the values reported in the other experiments could be lower than the actual value of σ either because of contamination or impurities or both. Nevertheless, σ may be actually

decreasing with increasing pressure by a small amount. A simple model allowing for such a possibility is presented in Section V.

The value of U has been found to be averaging around 0.36, and it is permissible as discussed in the kinetic model of Adt[9].

V. KINETIC THEORY MODEL OF CONDENSATION

V-1. Introduction

There have been many attempts to propose a theory explaining the decrease in value of condensation coefficient "σ" at increasing pressures, but none havebeen satisfactory. In this analysis, a kinetic theory model of the liquid and vapor phases has been developed to explain qualitatively the behaviour of condensation coefficient versus saturation pressure curve.

V-2. Model and Its Assumptions

This model has been developed for a liquid in equilibrium with its vapor at saturation temperature. The purpose of the model is to predict the condensation coefficient "σ" for the mass flux of the vapor incident on the liquid surface. The vapor molecules have been assumed to have a maxwellian velocity distribution.

The liquid molecules have stronger binding forces than the vapor molecules and are less free to move. As a result, the liquid molecules move slower than the vapor molecules at the same temperature. In the model, the liquid has been pictured to consist of particles which have effectively a higher mass than single-vapor molecules. These liquid particles can be imagined to be an aggregate of many molecules moving together. These particles are assumed to have the maxwellian velocity distribution. Only normal collisions have been taken into consideration. It has been assumed that there exists a potential well between the liquid and vapor, and the energy attributed to this well is the latent heat of

vaporization. The force of attraction has been assumed to be constant (Fig. 13) acting over a distance X over which the liquid particles and vapor molecules accelerate to achieve their final velocities before they collide. In other words, the potential energy of the well manifests itself in terms of kinetic energy of the liquid particle and vapor molecule. This conversion of potential energy to kinetic energy of liquid particle and vapor molecule is termed as "liquid particle and vapor molecule having fallen into the potential well."

The liquid particle has been assigned a mass "m" and velocity v_o, and the vapor molecule a mass M and velocity u_o. The positive directions of u_o and v_o are as shown in Fig. (12). The energy of the well is taken to be E. The value of E is expected to be of the order of h_{fg}, the latent heat of vaporization. In the calculations E has been set equal to h_{fg}. u_o and v_o are the respective velocities of the liquid particle and vapor molecule before the force of attraction has come into play. The collision is assumed to take place in the well, and after collision the velocity of the liquid particle is v_1 and that of the vapor molecule is u_1, while both are still in the well (Fig. (12)). The potential well has been pictured to be attached to the liquid particles.

V-3. Criterion for Sticking or Condensation

Let us suppose that the force of attraction "F" comes into play when the liquid particle and vapor molecule have come close enough (within a few molecule diameters). The force-distance diagram is as shown in Fig. (11).

$$\text{Then } F = m\frac{dv_o}{dt} \tag{V-3-1}$$

and

$$F = M\frac{du_o}{dt} \tag{V-3-2}$$

$$\therefore \frac{F}{m} + \frac{F}{M} = \frac{dv_o}{dt} + \frac{du_o}{dt} \tag{V-3-3}$$

$$= \frac{d(v_o + u_o)}{dt} \tag{V-3-4}$$

$$= \frac{d(V_{rel})}{dt} \quad . \tag{V-3-5}$$

The work done by this force over the distance X is

$$dE = F\cdot dX = \left(\frac{Mm}{M+m}\right)\frac{d(V_{rel})}{dt}\cdot dX \quad . \tag{V-3-6}$$

But $$V_{rel} = \frac{dX}{dt} \tag{V-3-7}$$

$$\therefore dE = F\cdot dX = \left(\frac{Mm}{M+m}\right) V_{rel}\, dV_{rel} \tag{V-3-8}$$

$$\therefore E = \int_o^X F\cdot dX = \left(\frac{Mm}{M+m}\right)\int_{V_{ri}}^{V_{rb}} V_{rel}\, dV_{rel} \tag{V-3-9}$$

where

V_{ri} = Initial relative velocity before the force F has come into play;

V_{rb} = Final relative velocity just before collision.

If the collision is considered completely elastic, the relative velocity just before the collision can be shown to be the same as after the collision from the conservation of momentum and energy; i.e. $v_{rb} = v_{rf}$.

$$\therefore E = \left(\frac{Mm}{M+m}\right)\left[\frac{V_{rf}^2}{2} - \frac{V_{ri}^2}{2}\right] \qquad \text{(V-3-10)}$$

In order that the liquid and vapor molecules stick to each other, they should not be able to come out of the potential well.

$\therefore$ The criterion for trapping is that

$$\frac{Mm}{M+m}\,\frac{V_{rf}^2}{2} < E \qquad \text{(V-3-11)}$$

because in that case they cannot have any real velocity after they come out of the potential well.

V-4. Expression for Coefficient of Condensation

The condensation coefficient has been defined as the ratio of the mass flux that condenses, to the total incident flux. In terms of our model, it is the ratio of the mass flux trapped in the potential well to the total incident mass flux under consideration.

$\therefore \sigma$ = condensation coefficient

$$= \frac{\text{trapped mass flux in the potential well}}{\text{total incident mass flux}}$$

The probability of a vapor molecule colliding with a liquid particle is proportional to the relative velocity between liquid particle and vapor molecule; i.e., the higher the relative velocity between them, the higher the probability of collision. Also, the collision probability depends upon the number of liquid particles with that relative velocity; i.e., the higher the number of particles with that relative velocity, the

higher is the probability of collision. Consequently, the probability of collision for a given vapor velocity u_o is as follows:

(Probability of collision) $\propto$ (Relative velocity between the liquid particle and vapor molecule) x (Velocity distribution function for liquid particles)

or $P_c(u_o) \propto (u_o + v_o)\ G(v_o)\ dv_o$. (V-4-1)

$G(v_o)\ dv_o$ is the maxwellian velocity distribution for the liquid particles.

For a given vapor velocity u_o, the minimum value for v_o is greater than $-u_o$ because if v_o is less than or equal to $-(u_o)$, the collision will never take place.

Out of all the collisions taking place for $-u_o < v_o < \infty$, only those will result in trapping of the vapor molecules which satisfy the criterion of trapping, i.e., for which

$$1/2\ \frac{Mm}{M+m}\ V_{rf}^2 \leq E \quad . \tag{V-3-11}$$

So for any value of v_o which is higher than that given by this relation, the trapping will not take place.

For a given u_o, the probability of trapping is therefore given by

$$p_t(u_o) = \frac{1}{N_1} \int_{-u_o}^{v_{o*}} (u_o + v_o)\ G(v_o)\ dv_o \tag{V-4-2}$$

where v_{o*} is the maximum value of v_o to satisfy Equation (V-3-11) for given u_o. N_1 is the normalization factor given by

$$N_1 = \int_{-u_o}^{\infty} (u_o + v_o)\, G(v_o)\, dv_o \qquad \text{(V-4-3)}$$

The velocity of vapor particle has also been assumed to have the maxwellian distribution. The condensation coefficient has been defined as the ratio of mass fluxes; therefore, in order to get an expression for the condensation coefficient, the probability of trapping for a given value of u_o has to be weighted both with respect to vapor velocity u_o and its distribution. The expression for condensation coefficient σ is, therefore, as follows:

$$\sigma = \frac{\int_o^{\infty} u_o\, f(u_o)\, du_o \int_{-u_o}^{v_{o*}} (u_o + v_o)\, G(v_o)\, dv_o}{\int_o^{\infty} u_o\, f(u_o)\, N_1\, du_o} \qquad \text{(V-4-4)}$$

$f(u_o)\, du_o$ [16] is also assumed to be a maxwellian distribution. Substituting for the distribution function, the expression for σ becomes

$$\sigma = \frac{\int_o^{\infty} u_o \sqrt{\frac{M}{2\pi\kappa T}}\, e^{-Mu_o^2/2\kappa T}\, du_o \int_{-u_o}^{v_{o*}} (u_o + v_o) \sqrt{\frac{m}{2\pi\kappa T}}\, e^{-mv_o^2/2\kappa T}\, dv_o}{\int_o^{\infty} u_o \sqrt{\frac{M}{2\pi\kappa T}}\, e^{-Mu_o^2/2\kappa T}\, du_o \int_{-u_o}^{\infty} (u_o + v_o) \sqrt{\frac{m}{2\pi\kappa T}}\, e^{-mv_o^2/2\kappa T}\, dv_o} \qquad \text{(V-4-5)}$$

which has been simplified in Appendix (B) to give

$$\sigma = \frac{\int_o^{\infty} \hat{u}_o\, e^{-\mu\hat{u}_o^2} \left[\left(e^{-\hat{u}_o^2} - e^{-\hat{v}_{o*}^2} \right) \frac{2}{\sqrt{\pi}} + 2\, \hat{u}_o (\operatorname{erf} \hat{v}_{o*} + \operatorname{erf} \hat{u}_o) \right] d\hat{u}_o}{\int_o^{\infty} \hat{u}_o\, e^{-\mu\hat{u}_o^2} \left[\left(e^{-\hat{u}_o^2} \right) \frac{2}{\sqrt{\pi}} + 2\, \hat{u}_o\, (1 + \operatorname{erf} \hat{u}_o) \right] d\hat{u}_o} \qquad \text{(V-4-6)}$$

where $$\hat{u}_o = u_o / \sqrt{\frac{2KT}{m}} \qquad \text{(V-4-7)}$$

$$\hat{v}_{o*} = v_{o*} / \sqrt{\frac{2KT}{m}} \quad . \qquad \text{(V-4-8)}$$

v_{o*} is a function of u_o as determined by the criterion of trapping as determined in the next section.

V.5 Determination of V_{o*}

To determine the value of v_{o*}, the conservation of momentum and energy has been invoked. If a completely elastic collision is considered, it can be shown that all the vapor molecules will be able to overcome the potential barrier, and so σ will always be zero. After the liquid particle and vapor molecule have entered the potential well, they share the energy E, corresponding to the potential well, between themselves, and if they do not lose a part of their kinetic energy, they will never be trapped, because they have had some energy to begin with, and extra energy E is contributed to their total energy by the potential well. Therefore, $\frac{1}{2} \frac{Mm}{M + m} V_{rf}^2$ will always be greater than E, and hence there will be no trapping of vapor molecules.

The loss of energy is attributed to inelasticity of collision. It has been assumed that kinetic energy of the system is not conserved, and on collision, the liquid particle which has been pictured to be an aggregate of many molecules could absorb a fraction of the total kinetic energy, involved in the collision, in terms of its internal energy. It is suspected, however, that the collision takes place over a very short interval of time, and forces involved in the collision are much higher

than the inter-molecular forces which exist in reality. They have been neglected in the model, and liquid particle has been modeled to be a free particle. Hence the assumption of conservation of momentum is a reasonable one. The energy absorbed by the liquid particle could later on be passed over to subsequent layers of liquid.

The model is as shown in Fig. (12). Conservation of momentum gives us

$$- m v_o + M u_o = + m v_1 - M u_1 \quad . \tag{V-5-1}$$

To take into effect the inelasticity of collision, a factor η is defined as follows

$$\eta = \frac{\text{total kinetic energy after the collision}}{\text{total kinetic energy before the collision}}$$

$$\therefore \eta = \frac{1/2\ m v_1^2 + 1/2\ M u_1^2}{1/2\ m v_o^2 + 1/2\ M u_o^2 + E} \quad . \tag{V-5-2}$$

The Equations (V-5-1) and (V-5-2) are solved for u_1 and v_1 to obtain

$$u_1 = \frac{(v_o - \mu u_o) + \sqrt{(u_o + v_o)^2 + (1 + \mu)\ [2\eta E/M - (1 - \eta)(\frac{v_o^2}{\mu} + u_o^2\ ]}}{1 + \mu} \tag{V-5-3}$$

$$v_1 = \frac{-(v_o - \mu u_o) + \mu \sqrt{(u_o + v_o)^2 + (1 + \mu)\ [2\eta E/M - (1 - \eta)(\frac{u_o^2}{\mu} + u_o^2)]}}{1 + \mu} \quad . \tag{V-5-4}$$

Applying the criterion of trapping to calculate the value of v_{o*} for a given u_o, we end up with

$$\frac{1}{2}\left(\frac{Mm}{M+m}\right) v_{rf}^2 = E \qquad \text{(V-5-5)}$$

$$\therefore (v_1 + u_1)^2 = \frac{2E}{M}(1+\mu) \qquad \text{(V-5-6)}$$

$$(u_o + v_{o*})^2 + (1+\mu)\left[2\eta\frac{E}{M} - (1-\eta)\left(\frac{v_o^2}{\mu} + u_o^2\right)\right]$$

$$= \frac{2E}{M}(1+\mu) \qquad \text{(V-5-7)}$$

$$(u_o + u_{o*})^2 = (1+\mu)(1-\eta)\left[\frac{2E}{M} + \frac{v_{o*}^2}{\mu} + u_o^2\right] \qquad \text{(V-5-8)}$$

from where v_{o*} can be calculated.

V-6. Calculation of σ

Numerical integration in Equation (V-4-6) is performed to calculate the value of σ. μ is chosen as a parameter, and curves are plotted for σ vs saturation pressure corresponding to various temperatures. To calculate the value of v_{o*}, η is required and that was calculated from the boundary condition that $\sigma = 1$ at $P = 0.004$ atmosphere which both the experiments and existing theories prove.

For each value of μ there exists a value of η to match $\sigma = 1$ at $P = 0.004$ atmosphere, and this set of μ and η is used for further σ calculations at higher temperatures and pressures. The results are as plotted in Fig. (14).

V-7. Checking of Assumption $\mu < 1$

It is proposed to check the assumption whether to assume that $\mu < 1$ is reasonable or not. As the vapor molecule approaches the liquid surface and the force of attraction comes into play, it actually is having interaction with many liquid molecules. The attraction forces are long-range forces, and repulsion forces are short-range forces. To a vapor molecule coming towards the liquid surface, the whole surface could look like a sea with ripples because of various modes of vibration of individual molecules, and these could present an overall averaged effect. As the vapor molecule comes nearer, however, the number of liquid molecules affecting the vapor molecule's acceleration reduces because the one nearest will have more effect than the ones far away.

The actual detailed surface condition could affect the nature of collisions, but it is a very complicated mechanism by which the collision occurs. More so because the process of attraction which occurs is long range, whereas the repulsion process is short range and more likely to be influenced the most by the one liquid molecule with which the collision takes place.

The criterion to check the assumption of $\mu < 1$ is whether the time of collision is short compared to that taken by the sound wave to transmit the energy to the molecules more deeply into the surface, because the minimum time taken to travel any distance by a wave is that taken by sound wave, and the number of intermolecular spacings

that the sound wave could travel in the duration of collision will determine the maximum number of liquid molecules affected.

In the kinetic model presented, we have assumed the liquid particles to be acting as an aggregate of single molecules acting together, and this type of check will give us an upper limit on the number of single molecules that could be assumed to be taking part in the collision with one vapor molecule.

Suppose ρ is the density of the liquid and a is the lattice spacing (Fig. (15)). Then (calculation has been made for sodium):

$$\rho = \frac{M_{Na}}{a^3} \qquad (V\text{-}7\text{-}1)$$

where

M_{Na} = mass of sodium molecule

a^3 ≃ volume/molecule in the lattice

$$\therefore a \simeq \left(\frac{M_{Na}}{\rho}\right)^{1/3} = \left[\frac{23}{6.02 \times 10^{23} \times 46 \times 0.016}\right]^{1/3} = 3.8 \times 10^{-8} \text{ cm} .$$

Suppose R_I is the radius of influence which the sound wave travels during the period in which the collision takes place;

$$\therefore R_I = c\tau \qquad (V\text{-}7\text{-}2)$$

where C = speed of sound in the liquid and τ is the time of collision.

$$\tau = \ell / v_{rb} \qquad (V\text{-}8\text{-}2)$$

where v_{rb} is the net relative velocity between the colliding particles and ℓ is the same characteristic length to determine the collision time. Since not much can be said about the exact value of ℓ, it is assumed that $\ell \approx a$, the lattice dimension.

Combining Equations (V-7-2) and (V-7-3), we get

$$R_I = a \cdot (\ell/a) \cdot (C/v_{rb}) \quad . \tag{V-7-4}$$

In Equation (V-7-4), v_{rb} depends on temperature, and so R is a function of temperature.

The number of molecules influenced are the ones within this radius of influence; therefore, the expression for the number of influenced molecule n can be written as

$$n \approx \frac{2\pi}{3} R_I^3/a^3 = \frac{2\pi}{3} \left[\frac{\ell}{a} \left(\frac{C}{v_{rb}}\right)\right]^3 \tag{V-7-5}$$

where v_{rb} is the relative velocity before collision. For an elastic collision, i.e., $\eta = 1$, the relative velocity before and after the collision will be the same. Using Equation (V-5-4) and (V-5-5), we have

$$v_{rb} = \sqrt{(u_s + v_o)^2 + (1 + \mu) \frac{2E}{M}} \quad . \tag{V-7-6}$$

Calculating at T = 1500 ^{o}R, we have

$$v_{rb} \simeq 9000 \text{ ft/sec.} \tag{V-7-7}$$

$$\therefore \frac{C}{v_{rb}} \approx 1;$$

therefore, substituting this value of C/v_{rb} in Equation (V-7-5), we see that

$$n \simeq \frac{2\pi}{3} \quad .$$

This is a simple order of magnitude analysis, and detailed molecular interactions have not been taken into account. Not much can be said about ℓ, and the value of n obtained above does not establish whether the assumption $\mu < 1$ is reasonable or not.

It is recommended to make then a detailed analysis of collision mechanism to check the assumption and thereby improve the kinetic model accordingly, incorporating these results.

VI. CONCLUSIONS

In the present investigation, it was found that the evaporation or condensation coefficient σ measured during the steady-state evaporation experiment is higher than that reported previously in condensation experiments. It was also found that impurities in the liquid could cause the value of σ to decrease. Similarly surface contamination (Adt[9]) and the presence of non-condensable gases (Kroger[5]) resulted in lower values of σ. This suggests that the contamination in the evaporation experiment was maintained at a lower level than that attained during the condensation experiments.

The results also suggest that σ measured during evaporation may not decrease with increasing values of saturation pressures corresponding to interface temperature. However, there is also a possibility of σ decreasing with increasing pressures, at a rate much smaller than that suggested by condensation data. The plots of σ versus saturation pressure, obtained from the kinetic theory model in Section V, lends support to this possibility.

The average values of transport coefficient U was measured to be 0.36. Schrage[6] assumed incident velocity distribution to be half maxwellian. Comparing his equation for rate of phase change, (I-3-5), with that obtained by Bornhorst[8], (I-4-1), we find that for his velocity distribution to be exact, U has to be equal to unity. Since the value of U measured from the experiment is different from unity, it suggests that actual incident velocity distribution may be a distorted half maxwellian.

VII. RECOMMENDATIONS

The evaporation data obtained so far is insufficient to lead to any firm conclusion regarding the behaviour of evaporation or condensation coefficient σ, at higher values of interface temperature. Both possibilities of σ remaining constant or decreasing with increasing values of interface temperature are still open. It is thus recommended to carry out steady-state evaporation at higher values of interface temperatures to ascertain the behaviour of σ at increasing interface temperatures.

The transport coefficient U should be predicted from a theoretical analysis employing Boltzmann's equation. This would give a basis to compare the experimental results. The method of describing kinetics (Reference (9)) employing an equilibrium distribution and a correction term could thus be avoided.

The kinetic model should be checked for the assumption $\mu < 1$ taking into account the binding intermolecular forces in greater detail, and the kinetic model should be improved accordingly.

BIBLIOGRAPHY

1. Nusselt, W. Zeitsch. d. ver. deutsch. Ing. 60, 541 (1916).

2. Sparrow, E. M. and Gregg, J. L., Trans. ASME, Jour. Ht. Transfer, Series C, 1959, pp. 13-18, including discussion by R. A. Seban.

3. Chen, M. M., Trans. ASME, Jour. Ht. Transfer, Series C, 83, 48-60 (Feb. 1961).

4. Koh, J. C. Y., et al., Int. Jour. Ht. and Mass Trans., 2, 69-82, March 1961.

5. Kroger, D. G., "Heat Transfer During Film Condensation of Potassium Vapor," Sc.D. Thesis, M.I.T., Sept., 1966.

6. Schrage, R. W., A Theoretical Study of Interphase Mass Transfer, Columbia University Press, New York, (1953).

7. Sukhatme, S. and Rohsenow, W., "Heat Transfer During Film Condensation of a Liquid Metal Vapor," Report No. 9167-27, Dept. of Mech. Eng'g., M.I.T., April, 1964.

8. Bornhorst, W. J., "Irreversible Thermodynamics of a Phase Change," Ph.D. Thesis, M.I.T., June 1966.

9. Adt, R. R., "A Study of Liquid-Vapor Phase Change of Mercury Based on Irreversible Thermodynamics," Sc.D. Thesis, M.I.T., June 1967.

10. Kennard, E. H., Kinetic Theory of Gases, McGraw-Hill Book Co., Inc., New York, 1938.

11. Teagon, W. P., "Heat Transfer and Density Distribution Measurements Between Parallel Plates in the Transition Region," Doctoral Thesis, M.I.T., June 1967.

12. Ditschburn, R. W. and Gilmour, J. C., "The Vapor Pressures and Monatomic Vapors," Rev. Mod. Phys., Vol. 13, Oct. 1941.

13. The International Nickel Co., Inc., Technical Bulletin T-15.

14. Weathergood, W. D., Jr., Tyler, J. C., and Ku, P. M., "Properties of Inorganic Energy-Conversion and Heat-Transfer Fluids for Space Applications," WADD Technical Paper 61-96, Nov. 1961.

15. Knudson, M., The Kinetic Theory of Gases, Metheun and Co. and John Wiley and Sons, Inc., New York, 1950.

16. Vincenti, W. G. and Kruger, C. H., Jr., Introduction to Physical Gas Dynamics, John Wiley and Sons, Inc., New York, 1965.

17. Subbotin, V. I., Ivanovsky, M. N., Sorokin, V. P., Chulkov, V. A., Teplofizilka Vysokih Temperatur, No. 4, (1964).

18. Barry, R. E., Ph.D. Thesis, University of Michigan, (1965).

19. Misra's data are presented by:
Wilhelm, D. J., "Condensation of Metal Vapors: Mercury and the Kinetic Theory of Condensation," ANL-6948, (1964).

20. Aladyev, I. T., et al., "Thermal Resistance of Phase Transition with Condensation of Potassium Vapor," Proceedings of the Third International Heat Transfer Conference, (1966).

21. Labuntsov, P. A. and Smirnov, S. I., "Heat Transfer in Condensation of Liquid Metal Vapors," Proceedings of the Third International Heat Transfer Conference, (1966).

22. Kline, S. J. and McClintock, F. A., "Describing Uncertainties in Single-Sample Experiments," Mechanical Engineering, Vol. 75, January, 1953.

APPENDIX A - CONSIDERATION OF EXPERIMENTAL ERRORS

A-1. Uncertainty Intervals

The method suggested by Kline and McClintock[22] is used to present the uncertainties incurred in the experiment. These uncertainties are an indication of the reliability of the results obtained. The uncertainty interval ω_X for a quantity $X(\nu_i)$ is computed from

$$\omega_X = \sqrt{\sum_{\nu_i} \left(\frac{\partial X}{\partial \nu_i}\, \omega_{\nu_i}\right)^2} \qquad \text{(A-1)}$$

where the sum is over the quantities ν_i upon which the result X depends, and ω_{ν_i} is the estimated error in quantity ν_i. The values of ω_{ν_i} used are left up to the rational judgment of the observer. The results thus obtained indicate the credibility of this judgment.

A-2. Important Errors in U

From the expression for U (Equation (II-3-6)), it is found that the major sources of error are contributed by the errors in the vapor temperature T_g and the liquid interface temperature T_{fi}. The error in T_{fi} is mainly due to errors in T_{NI} and h_{Hg}. Substituting these three major sources of error in (A-1), we obtain

$$\omega_U = U \sqrt{\left(\frac{\omega_{T_g}}{\delta T}\right)^2 + \left(\frac{\omega_{T_{NI}}}{\delta T}\right)^2 + \left(\frac{(\Delta T/\Delta X)_{Hg}}{\delta T}\, \omega_{h_{Hg}}\right)^2} \,. \qquad \text{(A-2)}$$

In terms of the symbols used in Table II, Equation (A-2) can be written as

$$TPEU = \omega_U / U \tag{A-3}$$

or

$$TPEU = \sqrt{(PEUTG)^2 + (PEUTN)^2 + (PEUHHG)^2} \; . \tag{A-4}$$

The error in the vapor temperature is estimated from the differences in the temperatures measured by the thermocouples in the vapor and is found to be $\pm$ 0.2 - 0.3 ^{o}F.

The error in T_{NI} is estimated to be the difference in the values of T_{NI} computed from four and five point least square, straight lines drawn through the temperatures measured in the nickel block. Both the errors in T_{NI} and T_{gi} are found to be close to that found in the thermocouple calibration which is $\pm$ 0.2 ^{o}F. The error in the liquid depth is taken to be $\pm$ 0.0015" for all the data.

A-3. Important Errors in σ

In the experiment, the term $\frac{\delta T}{2T}$ is found to be very small compared to $\frac{\delta P}{P}$, and so the Equation (II-3-6) can be rewritten as

$$\frac{2\sigma}{2 - \sigma} = (J_i)_{ss} \frac{\sqrt{2\pi RT}}{(\delta P)_{ss}} \tag{A-5}$$

Taking into account the important sources of error in σ, which are expected to be the errors in P_g, T_{NI}, and h_{Hg}, we obtain

$$\omega_\sigma = \sigma\left(\frac{2-\sigma}{2}\right)\sqrt{\left(\frac{\omega_{P_g}}{P}\right)^2 + \left(\frac{\partial P_s}{\partial T_{fi}}\,\frac{\omega_{T_{NI}}}{\delta P}\right) + \left(\frac{\partial P_s}{\partial T_{fi}}\left(\frac{\Delta T}{\Delta X}\right)_{Hg}\frac{\omega_{h_{Hg}}}{\delta P}\right)^2} \qquad \text{(A-6)}$$

where $\frac{\partial P_s}{\partial T_{fi}}$ is the slope of the saturation pressure-temperature curve of mercury. In terms of symbols used in Table II, Equation (A-6) becomes

$$TPE\sigma = \frac{\omega_\sigma}{\sigma} \qquad \text{(A-7)}$$

or

$$TPE\sigma = \sqrt{(PE\sigma HG)^2 + (PE\sigma TNI)^2 + (PE\sigma HHG)^2}\ .$$

The error in the system pressure P_g is taken to be 0.02 inch of water. This accounts for the error in reading the manometer. The least count of the vernier scale is 0.01 inch.

A-4. Additional Errors

Besides the errors stated above, there are many other sources of error which are expected to be small. The errors due to incorrect values of material properties are expected to be small compared to quantities measured. The saturation pressure-temperature data are accurate up to 22[13]. There is a possibility of an error due to a non-linear temperature profile in the liquid layer. The tests were run at different combinations of liquid depth and temperature gradients, and the range of Grashoff number was noted to be quite wide; however, no systematic error was detected.

The error due to thermal contact resistance at mercury-nickel interface should be negligible for a clean wetted surface. But any such error will cause liquid interface temperature T_{fi} and hence corresponding saturation pressure, $P_s(T_{fi})$ to be lower than that used in the present calculation. This would result in lower values of both δT and δP thereby yielding smaller values of U and larger values of σ.

The error in the manometer reference pressure is estimated from the reading of a vacuum thermocouple gage to be 0.01 inch of water and is included in the upper bound on σ in Fig. (10).

APPENDIX B - EVALUATION OF INTEGRAL APPEARING IN EQUATION (V-4-5)

In this appendix the part of the integral used in Equation (V-4-5) has been evaluated

$$I = \int_{-u_o}^{v_{o*}} (u_o + v_o) \sqrt{\frac{m}{2\pi\kappa T}}\, e^{-mv_o^2/2\kappa T}\, dv_o$$

$$= \int_{-u_o}^{o} u_o \sqrt{\frac{m}{2\pi\kappa T}}\, e^{-mv_o^2/2\kappa T}\, dv_o + \int_{-u_o}^{o} v_o \sqrt{\frac{m}{2\pi\kappa T}}\, e^{-mv_o^2/2\kappa T}\, dv_o$$

$$+ \int_{o}^{v_{o*}} u_o \sqrt{\frac{m}{2\pi\kappa T}}\, e^{-mv_o^2/2\kappa T} \cdot dv_o + \int_{o}^{v_{o*}} v_o \sqrt{\frac{m}{2\pi\kappa T}} \cdot e^{-mv_o^2/2\kappa T} \cdot dv_o$$

$$= I_1 + I_2 + I_3 + I_4$$

where

$$I_1 = \int_{-u_o}^{o} u_o \sqrt{\frac{m}{2\pi\kappa T}} \cdot e^{-mv_o^2/2\kappa T} \cdot dv_o$$

$$= + \int_{o}^{u_o} u_o \sqrt{\frac{m}{2\pi\kappa T}} \cdot e^{-mv_o^2/2\kappa T} \cdot dv_o$$

$$I_2 = \sqrt{\frac{m}{2\pi\kappa T}} \int_{-u_o}^{o} v_o\, e^{-mv_o^2/2\kappa T}\, dv_o$$

$$= - \sqrt{\frac{m}{2\pi\kappa T}} \int_{o}^{u_o} v_o\, e^{-mv_o^2/2\kappa T} \cdot dv_o$$

$$I_3 = \int_o^{v_{o*}} u_o \sqrt{\frac{m}{2\pi\kappa T}}\, e^{-mu_o^2/2\kappa T} \cdot dv_o$$

$$I_4 = \int_o^{v_{o*}} v_o \sqrt{\frac{m}{2\pi\kappa T}} \cdot e^{-mv_o^2/2\kappa T} \cdot dv_o \quad .$$

In all these integrals, only v_o is the variable.

$$I_1 = \int_o^{u_o} u_o \sqrt{\frac{m}{2\pi\kappa T}}\, e^{-mv_o^2/2\kappa T} \cdot dv_o$$

$$= u_o \sqrt{\frac{m}{2\pi\kappa T}} \left[\operatorname{erf} \frac{u_o}{\sqrt{\frac{2\kappa T}{m}}}\right] \cdot \sqrt{\frac{2\kappa T}{m}} \quad \frac{\sqrt{\pi}}{2}$$

$$= \frac{1}{2} u_o \left[\operatorname{erf} \frac{u_o}{\sqrt{\frac{2\kappa T}{m}}}\right]$$

$$I_2 = - \int_o^{u_o} \sqrt{\frac{m}{2\pi\kappa T}} \cdot v_o\, e^{-mv_o^2/2\kappa T}\, dv_o$$

$$I_2 = - \sqrt{\frac{m}{2\pi\kappa T}} \int_o^{u_o} \frac{2\kappa T}{m} \cdot \frac{v_o}{\sqrt{\frac{2\kappa T}{m}}}\, e^{-mv_o^2/2\kappa T} \cdot \frac{dv_o}{\sqrt{\frac{2\kappa T}{m}}}$$

$$= - \sqrt{\frac{m}{2\pi\kappa T}} \left[\frac{2\kappa T}{m} \frac{1}{2}(1 - e^{-mu_o^2/2\kappa T})\right]$$

$$I_3 = \int_o^{v_{o*}} u_o \sqrt{\frac{m}{2\pi\kappa T}} \cdot e^{-mv_o^2/2\kappa T} \cdot dv_o$$

$$= u_o \sqrt{\frac{m}{2\pi\kappa T}} \left[\sqrt{\frac{2\kappa T}{m}} \cdot \left(\operatorname{erf} \sqrt{\frac{mv_{o*}^2}{2\kappa T}}\right)\right] \quad \frac{\sqrt{\pi}}{2}$$

$$I_4 = \int_0^{v_{o*}} v_o \sqrt{\frac{m}{2\pi\kappa T}} \cdot e^{-mv_o^2/2\kappa T} \cdot dv_o$$

$$= \sqrt{\frac{m}{2\pi\kappa T}} \left(\frac{2\kappa T}{m} \cdot \frac{1}{2}(1 - e^{-mv_{o*}^2/2\kappa T})\right)$$

$$\hat{u}_o = \frac{u_o}{\sqrt{\frac{2\kappa T}{m}}}$$

$$\hat{v}_{o*} = \frac{u_{o*}}{\sqrt{\frac{2\kappa T}{m}}}$$

$$I = I_1 + I_2 + I_3 + I_4$$

$$= \sqrt{\frac{m}{2\pi\kappa T}} \left[\hat{u}_o \left(\frac{2\kappa T}{m}\right) \frac{\sqrt{\pi}}{2} \operatorname{erf}(\hat{u}_o) - \frac{\kappa T}{m}(1 - e^{u_o^2})\right.$$

$$\left. + \hat{u}_o \left(\frac{2\kappa T}{m}\right) \frac{\sqrt{\pi}}{2} \operatorname{erf}(v_{o*}) + \frac{\kappa T}{m}(1 - e^{-\hat{v}_{o*}^2})\right]$$

$$= \sqrt{\frac{m}{2\pi\kappa T}} \left[\frac{2\kappa T}{m}\right]\left[\frac{\sqrt{\pi}}{2}\right]\left[\hat{u}_o[\operatorname{erf}(\hat{u}_o) + \operatorname{erf}(v_{o*})] + (e^{-\hat{u}_o^2} - e^{-v_{o*}^2}) \frac{1}{\sqrt{\pi}}\right] .$$

To calculate the value of N_1 for a given u_o, we substitute $v_{o*} = \infty$ in the value of I above

$$N_1 = I_{v_{o*}=\infty} = \sqrt{\frac{m}{2\pi\kappa T}} \left[\frac{2\kappa T}{m}\right] \frac{\sqrt{\pi}}{2} \left[\hat{u}_o(1 + \operatorname{erf}(\hat{u}_o)) + \frac{e^{-u_o^2}}{\sqrt{\pi}}\right] .$$

Substituting these values of I and N_1 in the Equation (V-4-5), we end up with

$$\sigma = \frac{\int_0^\infty \hat{u}_o \cdot e^{-\mu\hat{u}_o^2} \left\{[e^{-\hat{u}_o^2} - e^{-\hat{v}_{o*}^2}] + \sqrt{\pi} \cdot \hat{u}_o(\text{erf } \hat{v}_{o*} + \text{erf } \hat{u}_o)\right. d\hat{u}_o}{\int_0^\infty \hat{u}_o\, e^{-\mu\hat{u}_o^2} \left\{e^{-\hat{u}_o^2} + \hat{u}_o \sqrt{\pi}\ (\text{erf } \hat{u}_o + 1)\right\} d\hat{u}_o}$$

TABLE NO. 1

Test No.	Ps atm.	$-\delta P/P$	$-\delta T/T$	h_{Hg} in.	J_i lbm/ft^{2}hr	σ	U
1	0.01295	0.14018	0.00513	0.016	146.5	0.32	0.76
2	0.0127	0.10796	0.0069	0.019	146.5	0.41	0.72
3	0.0150	0.044	0.00246	0.025	194.7	0.82	0.32
4	0.0162	0.041	0.00181	0.015	194.1	0.81	0.26
5	0.0183	0.031	0.0015	0.020	140.1	0.75	0.33
6	0.0192	0.0313	0.0025	0.017	206.0	0.90	0.41
7	0.0176	0.0424	0.0024	0.025	206.0	0.79	0.37
8	0.0223	0.0256	0.00129	0.013	142.6	0.75	0.34
9	0.0219	0.0269	0.00154	0.019	140.1	0.73	0.40
10	0.0213	0.0257	0.00181	0.023	140.2	0.76	0.47
11	0.0262	0.0259	0.00124	0.026	158.0	0.72	0.34
12	0.0280	0.0255	0.00140	0.015	158.6	0.70	0.41

TABLE NO. 2

% Errors in U and σ*

Test No.	PEUTG	PEUTN	PEUHHG	TPEU	PEσPG	PEσTN	PEσHHG	TPEσ
1	5	.3	9	10	2	.14	4	5
2	7	1	10	12	3	.4	6	7
3	15	5	25	29	5	2	13	14
4	13	7	33	36	4	3	13	14
5	24	2	29	38	5	0.1	13	14
6	9	11	24	28	5	9	18	21
7	14	13	25	32	4	7	13	16
8	27	4	33	43	5	2	15	16
9	15	7	27	32	5	4	14	16
10	19	8	23	31	6	5	15	17
11	28	3	37	47	5	2	15	16
12	12	7	33	39	5	7	17	19

*Refer to Appendix A for Error Analysis

PEUTG = % error in U due to error in measuring T_g.

PEUTN = % error in U due to error in measuring T_{NI}.

PEUHHG = % error in U due to error in measuring h_{Hg}.

TPEU = total % error in U.

PEσPG = % error in σ due to error in measuring P_g.

PEσTN = % error in σ due to error in measuring T_{NI}.

PEσHHG = % error in σ due to error in measuring h_{Hg}.

TPEσ = total % error in σ.

TABLE NO. 3*

Test No.	σ_{max}	σ	σ_{min}	U_{max}	U	U_{min}
1	0.34	0.32	0.30	0.84	0.76	0.68
2	0.43	0.41	0.38	0.80	0.72	0.63
3	0.93	0.82	0.71	0.42	0.32	0.23
4	0.93	0.81	0.69	0.35	0.26	0.16
5	0.85	0.75	0.64	0.45	0.33	0.20
6	1.07	0.90	0.73	0.62	0.41	0.28
7	0.91	0.79	0.66	0.48	0.37	0.24
8	0.88	0.75	0.62	0.49	0.34	0.19
9	0.85	0.73	0.60	0.54	0.40	0.27
10	0.90	0.76	0.63	0.61	0.47	0.32
11	0.85	0.72	0.58	0.51	0.34	0.18
12	0.84	0.70	0.56	0.58	0.41	0.15

*

σ_{max}	maximum value of σ
σ	mean value of σ
σ_{min}	minimum value of σ
U_{max}	minimum value of U
U	mean value of U
U_{min}	minimum value of U

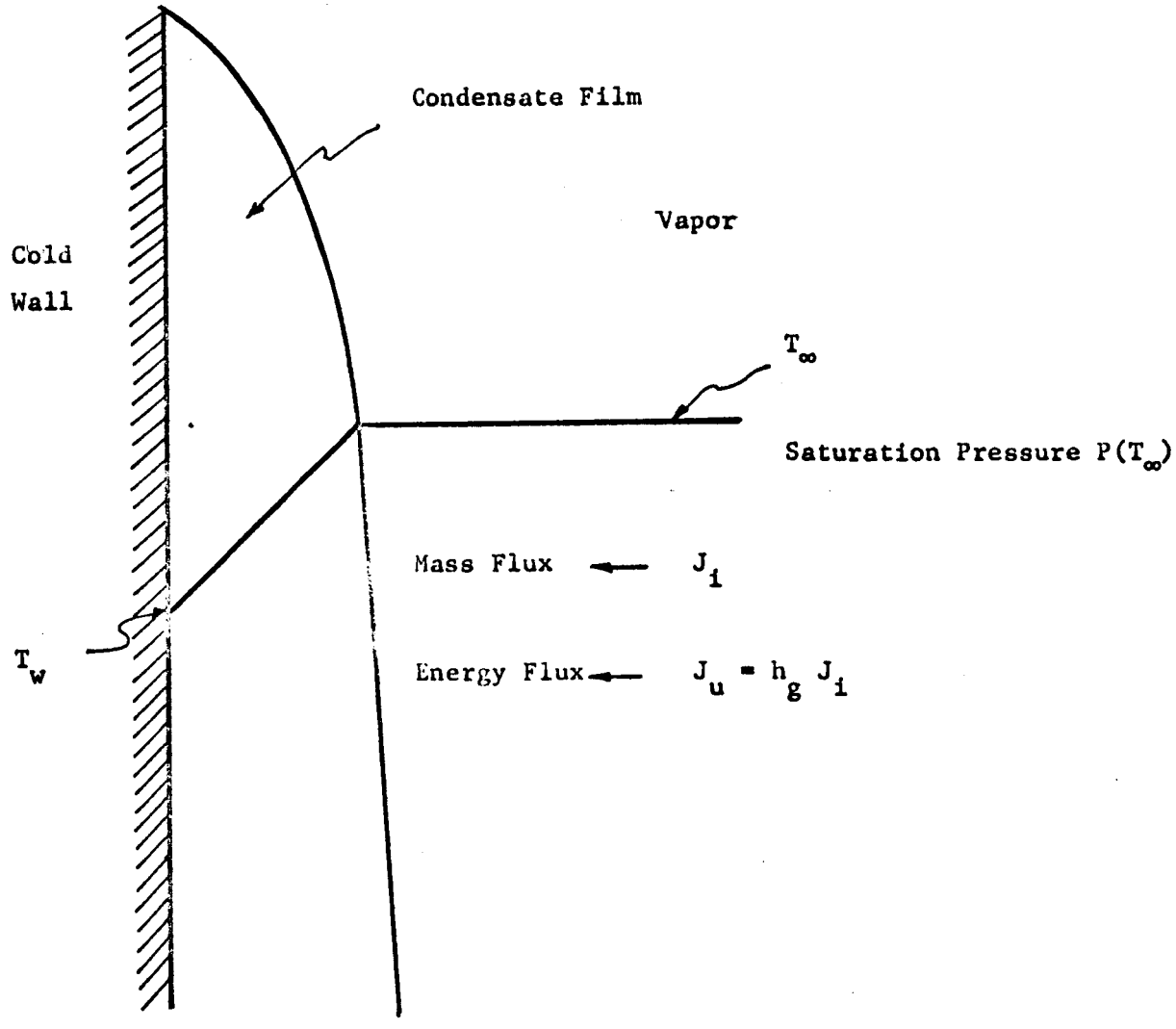

Figure 1 - Nusselt Model of Condensation

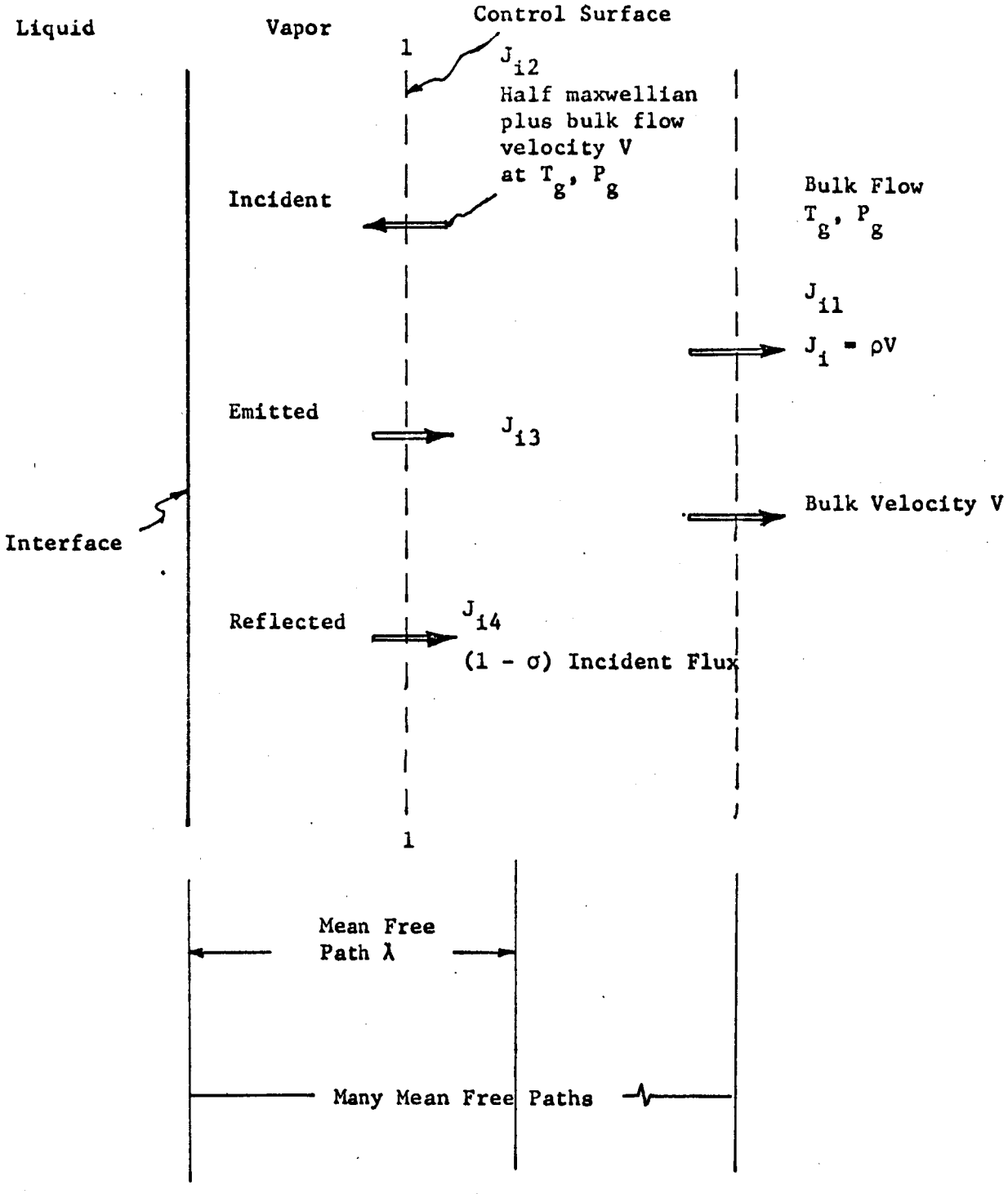

Figure 2 - Schrage's Kinetic Model of Phase Change

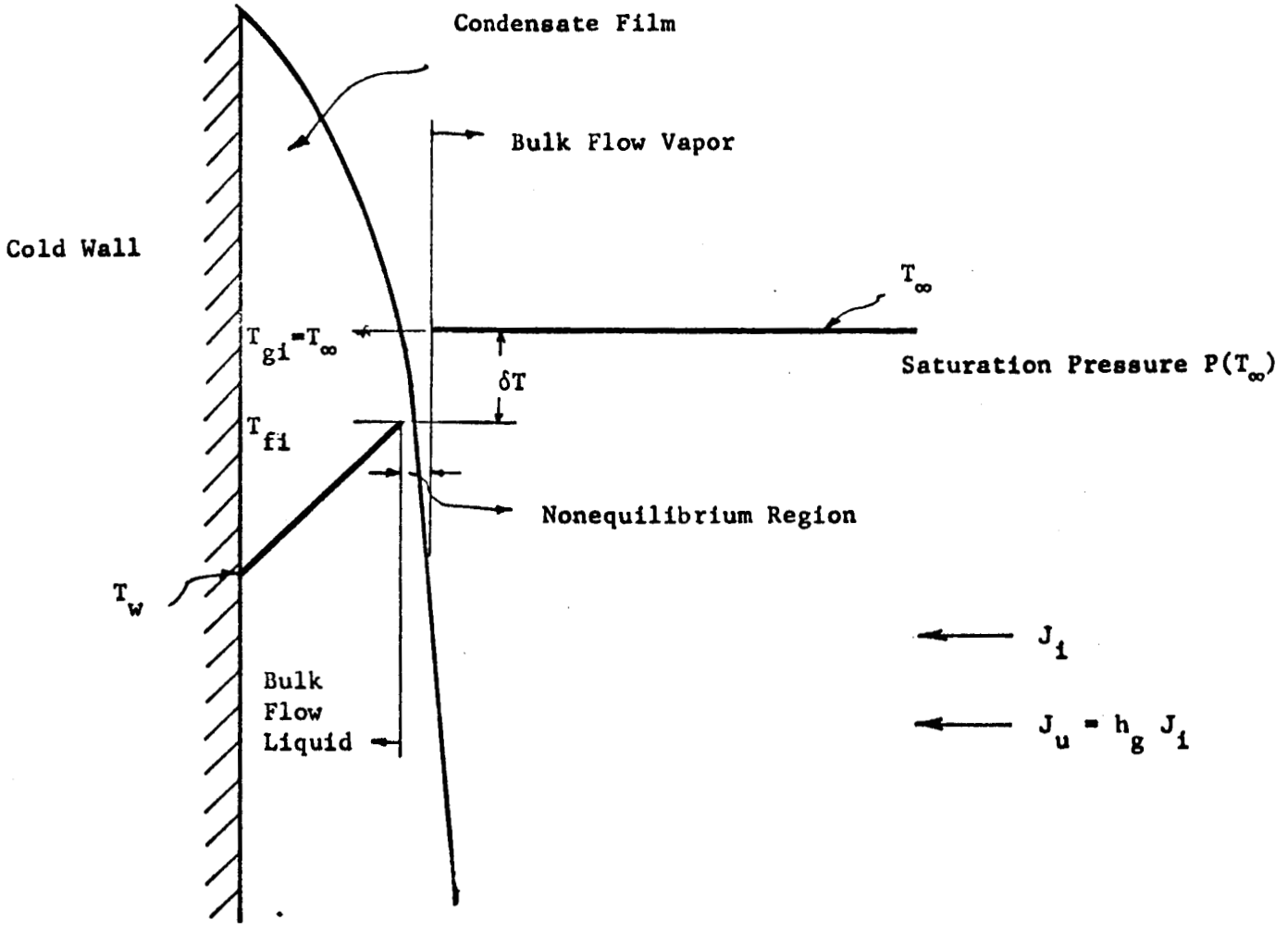

Figure 3 - Incorporation of Schrage's Kinetic Analysis in the Condensation Problem

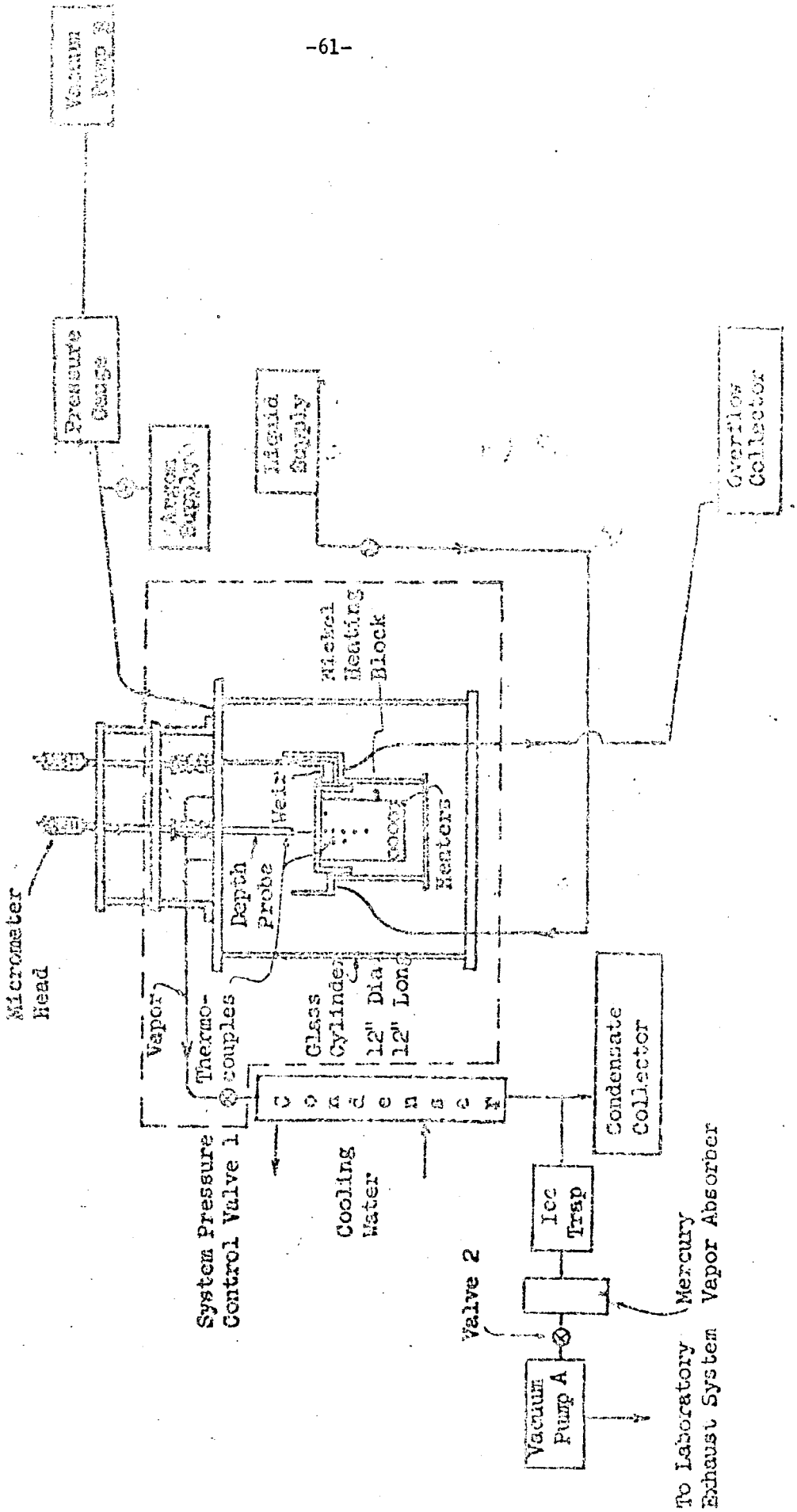

Figure 4 - Flow Diagram of Experiment

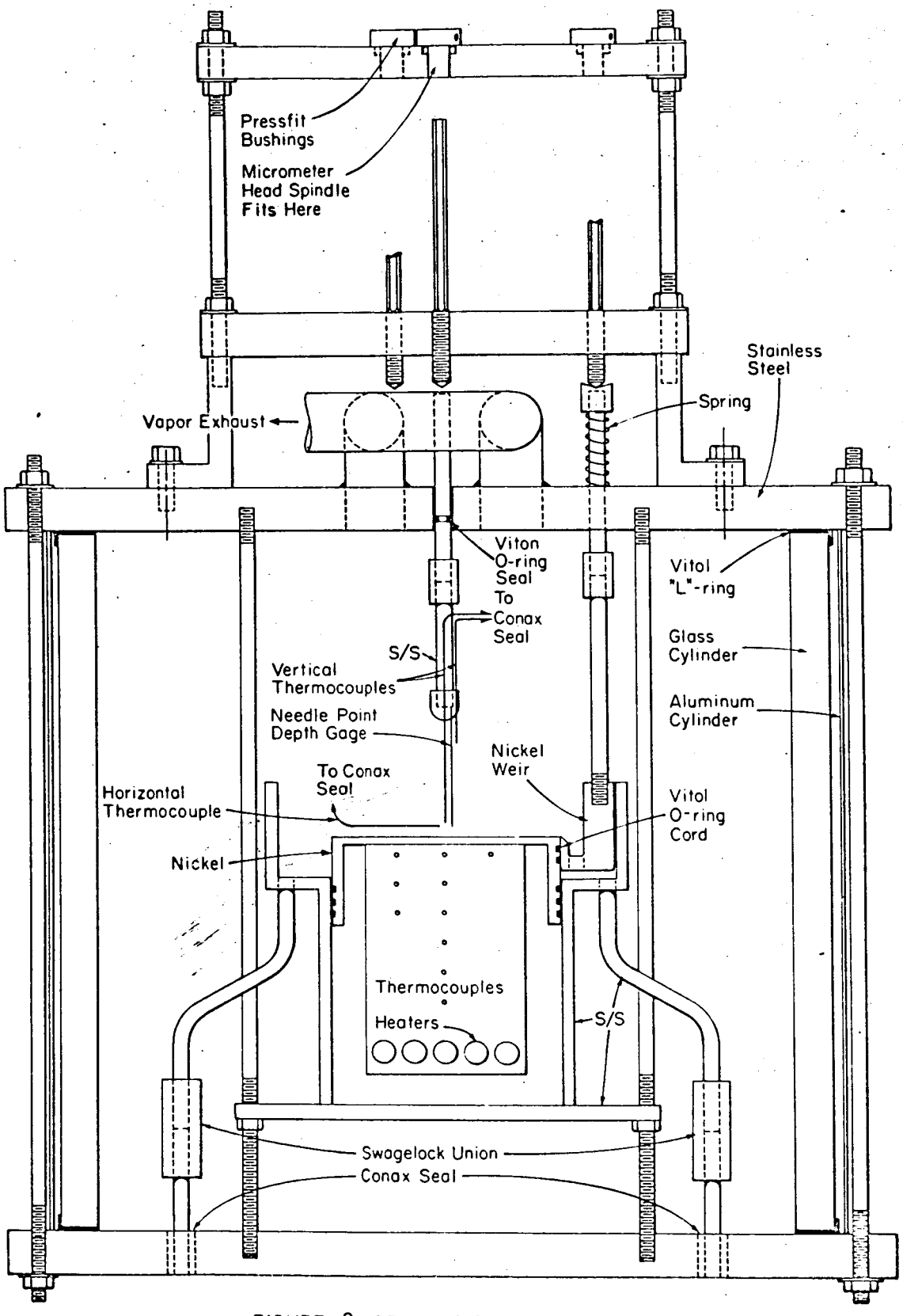

FIGURE 8 DRAWING OF TEST SECTION

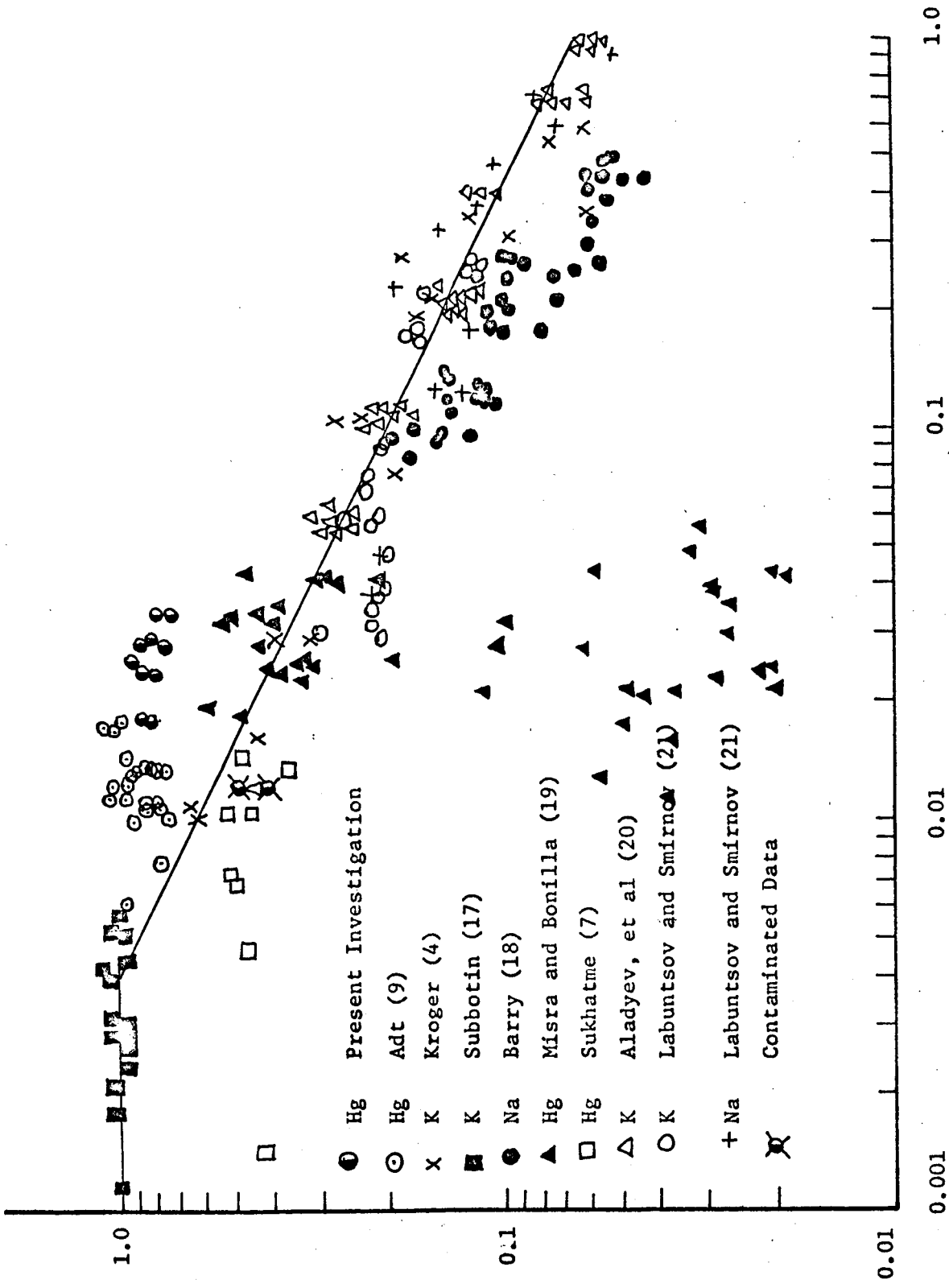

Figure 9 - Condensation Coefficient σ versus Pressure P_s for Various Liquid Metal

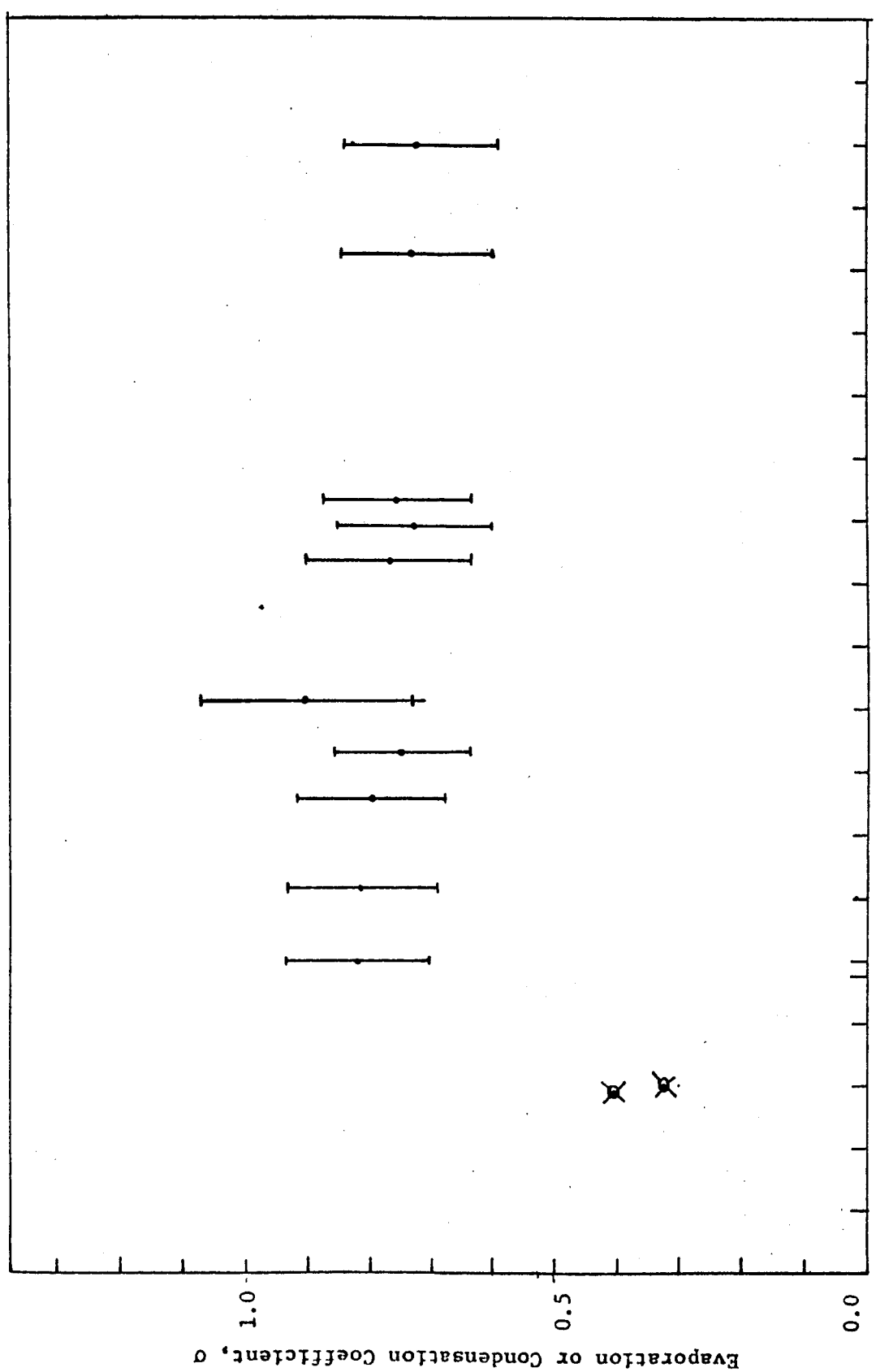

Figure 10 - Condensation Coefficient σ versus Pressure P_s for Steady State Evaporation Experiment

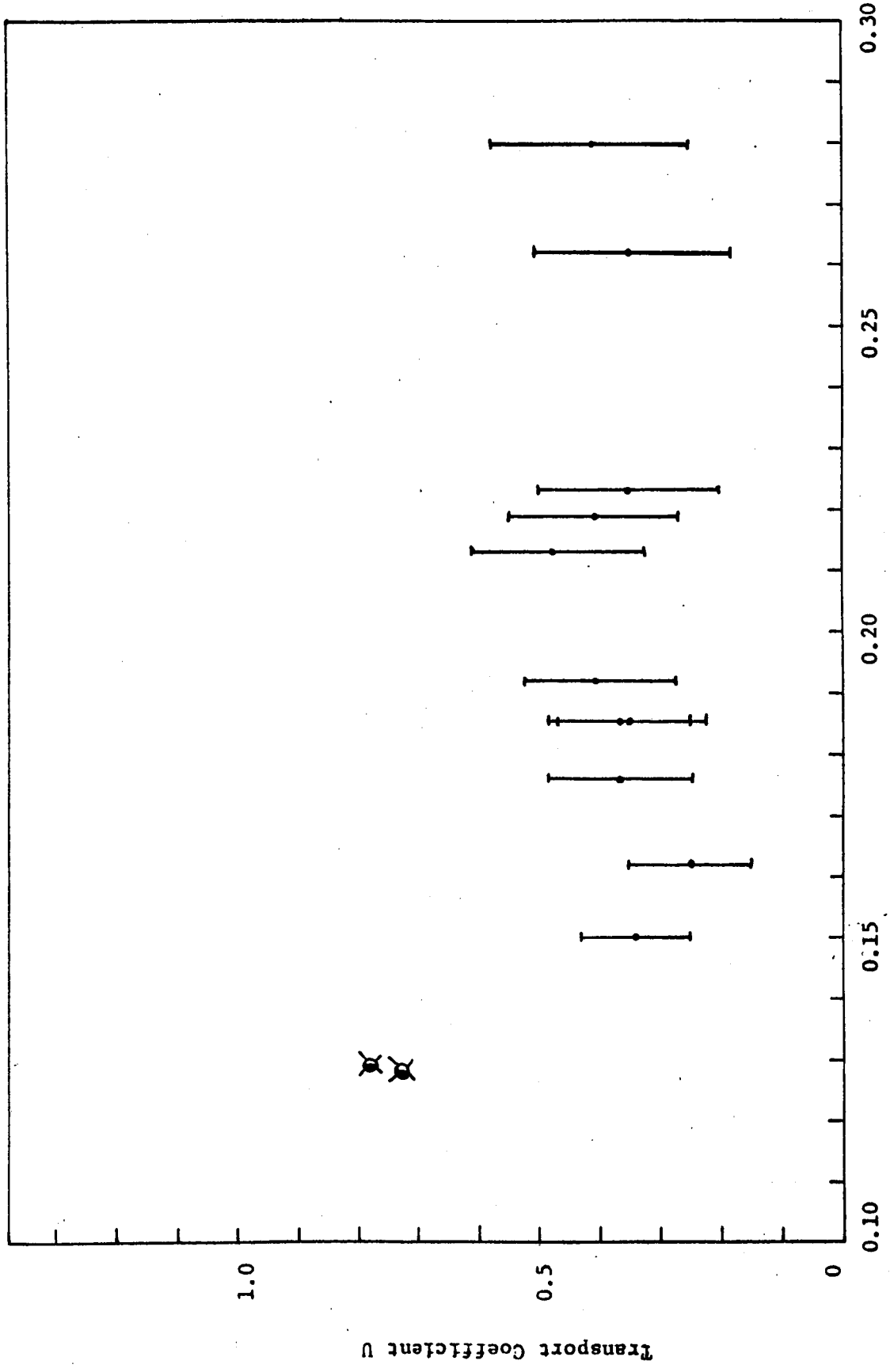

Figure 11 - Transport Coefficient U versus Pressure P_s for Steady State Evaporation Experiment

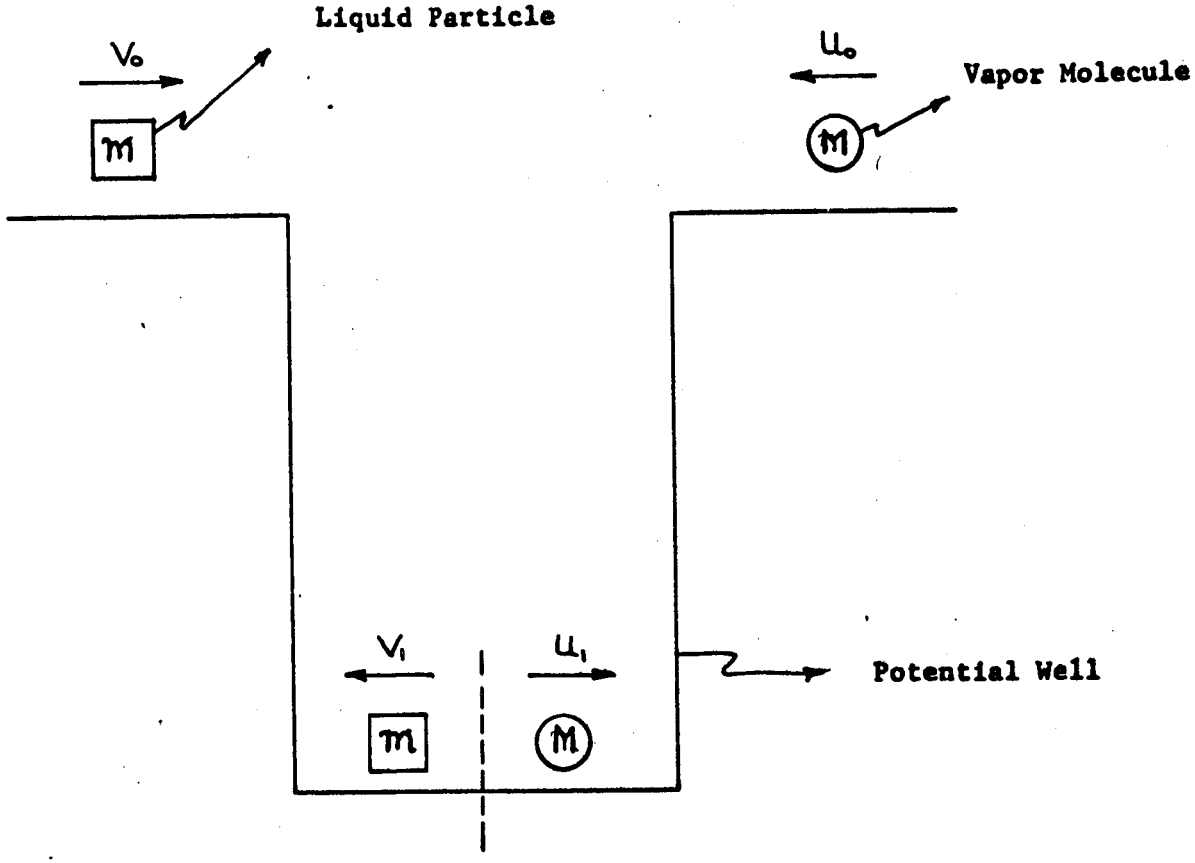

Figure 12 - Model Showing the Collision between the Liquid Particle and Vapor Molecule

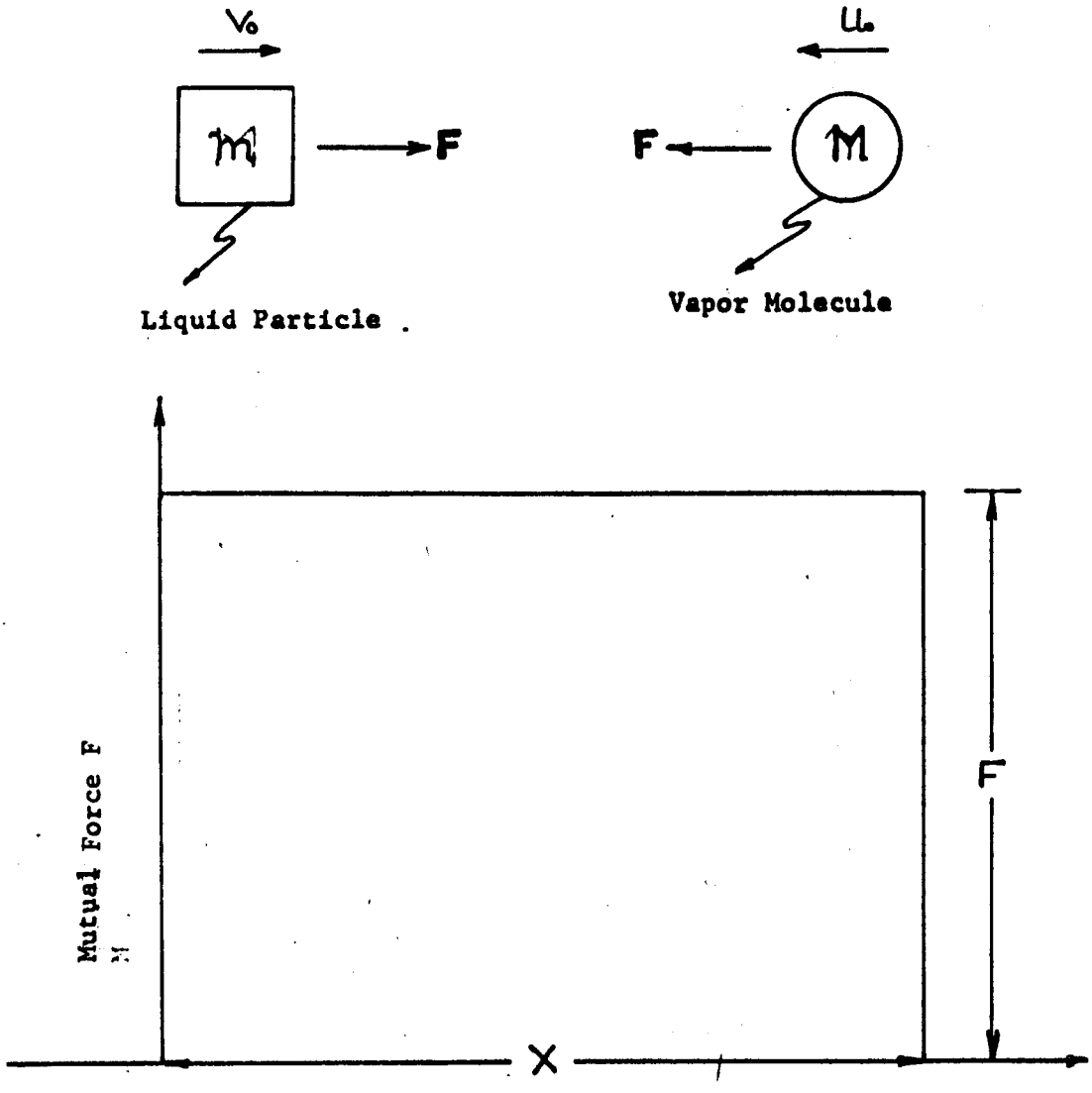

Figure 13 - Mutual Force between Liquid Particle and Vapor Molecule versus Relative Distance between Them

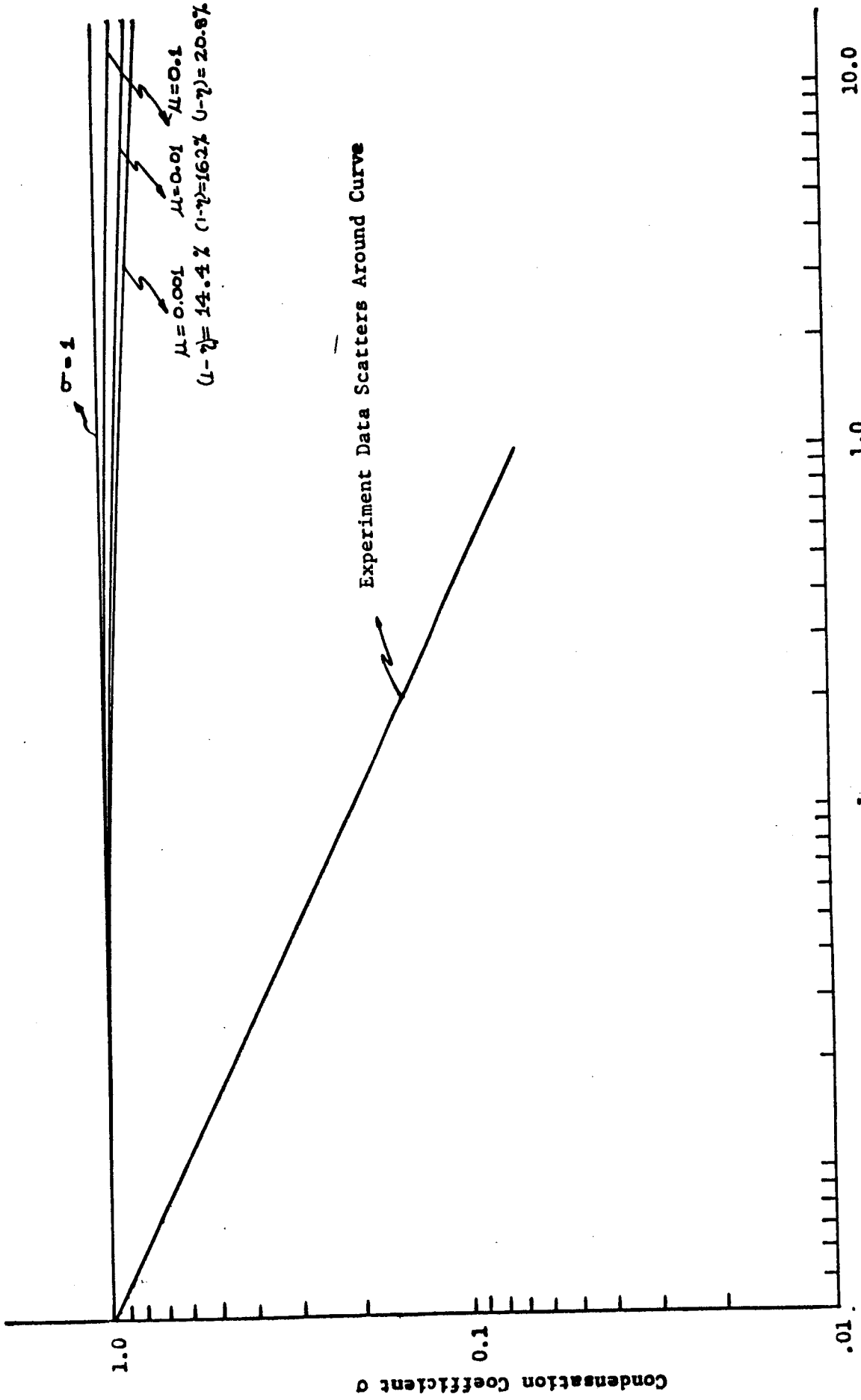

Figure 14 - Condensation Coefficient σ versus Pressure P_s as Predicted by Kinetic Theory Metal

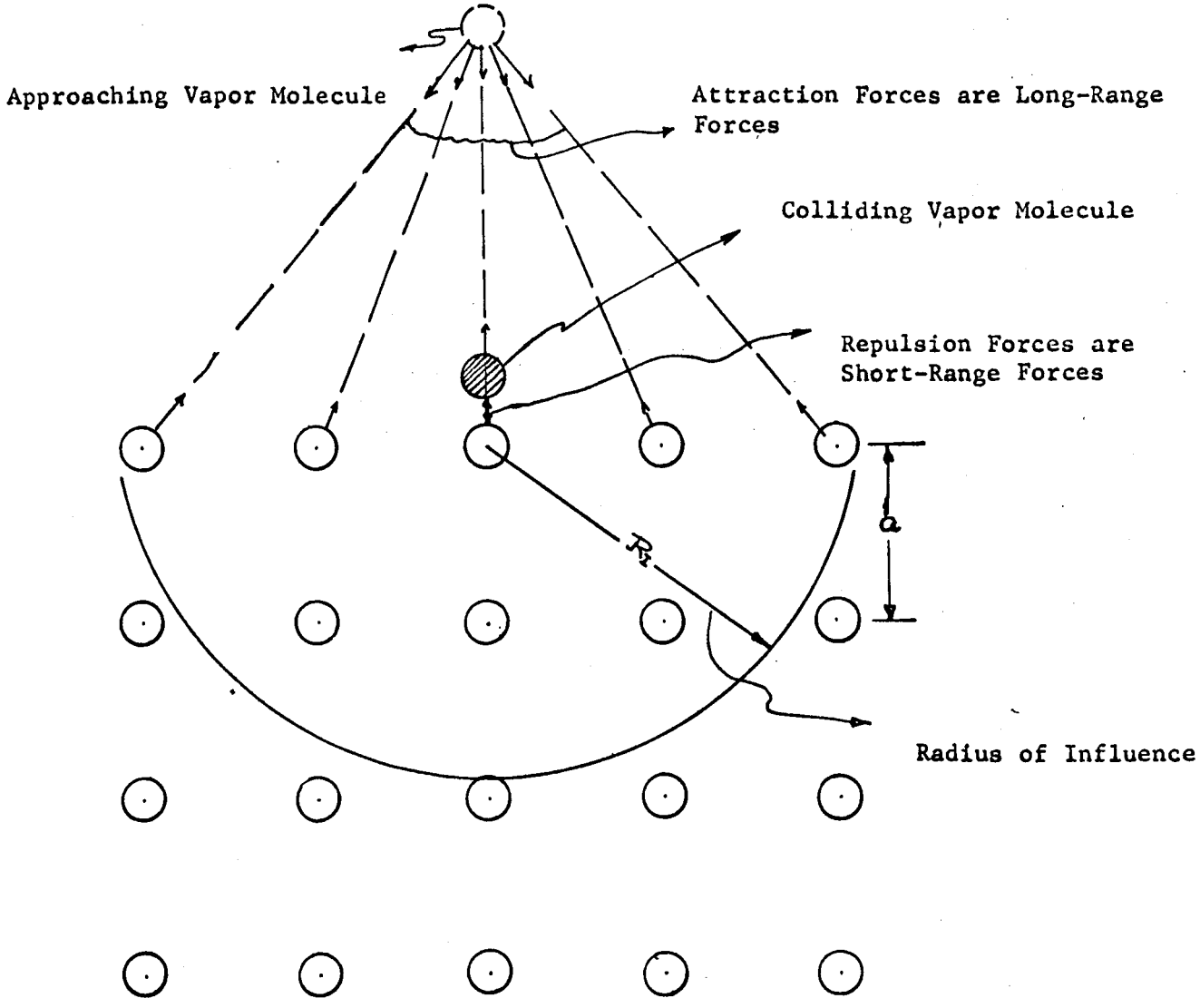

Figure 15 - Model for Checking Assumption $\mu < 1$ Showing a Collision of Vapor Molecule with a Molecule in Liquid Lattice